Superconvergent Functional Estimates from Tensor-Product Generalized Summation-by-Parts Discretizations in Curvilinear Coordinates

David A. Craig Penner · David W. Zingg

Abstract We investigate superconvergent functional estimates in curvilinear coordinates for diagonal-norm tensor-product generalized summation-by-parts operators. We show that interpolation/extrapolation operators of degree greater than or equal to $2p$ are required to preserve at least $2p$ quadrature accuracy and functional superconvergence in curvilinear coordinates when: (1) the Jacobian of the coordinate transformation is approximated by the same generalized summation-by-parts operator that is used to approximate the flux terms and (2) the degree of the generalized summation-by-parts operator is lower than the degree of the polynomial used to represent the geometry of interest. Legendre-Gauss-Lobatto and Legendre-Gauss element-type operators are considered. When the aforementioned condition (2) is violated for the Legendre-Gauss operators, there is an even-odd quadrature convergence pattern that is explained by the cancellation of the leading truncation error terms for the interpolation/extrapolation operators that correspond to the odd-degree Legendre-Gauss operators. The theory developed is confirmed through numerical examples with a steady one-dimensional problem and the unsteady two-dimensional linear convection equation.

D. A. Craig Penner
University of Toronto Institute for Aerospace Studies
E-mail: david.craigpenner@mail.utoronto.ca

D. W. Zingg
University of Toronto Institute for Aerospace Studies
E-mail: dwz@oddjob.utias.utoronto.ca

1 Introduction

Generalized summation-by-parts (SBP) methods, when combined with simultaneous approximation terms (SATs) [5,13,33], provide a provably linearly and nonlinearly stable, conservative, and consistent way to numerically solve a variety of linear and nonlinear partial differential equations (PDEs) [7,12, 34]. Initially developed to enable energy-stable finite-difference discretizations similar to those pioneered in the finite-element framework [25], SBP methods have been generalized [11] such that the SBP property can be applied to a broad class of high-order methods that includes some discontinuous Galerkin and flux reconstruction schemes [15,32].

In addition to being energy stable, an SBP scheme can be constructed to be dual consistent. Dual consistency is a concept that is widely understood in the context of Galerkin finite-element schemes, for example, which has enabled the development of schemes that exhibit functional superconvergence [6,16,28]. In general, a discretization is dual consistent if the discrete dual problem associated with the discretization is a consistent discretization of the continuous dual problem. For classical diagonal-norm SBP operators, if the discretization is dual consistent, then the underlying quadrature and solution functionals converge at the same rate as the order of the interior operator, i.e., $2p$, where p is the degree of the SBP operator [1,20,22]. A portion of these results have been extended to generalized SBP operators in the context of generalized SBP time-marching methods [2,3].

In practice, functionals are often the quantities of primary interest from a simulation, for example in aerodynamics, where forces and moments are frequently the most important quantities. These types of aerodynamic flows routinely involve complex geometries on curvilinear domains. Therefore, it is important to understand the impact of curvilinear coordinate transformations on functionals obtained through generalized SBP discretizations.

The primary objective of the present work is to extend the theory of functional superconvergence established in [2,3,20] for classical and generalized SBP operators to generalized SBP operators in curvilinear coordinates. To do this, we make the following contributions:

– We show that interpolation/extrapolation operators of degree $r \geq 2p$ are required to preserve at least $2p$ functional superconvergence under specific conditions.

– We identify and explain the even-odd functional convergence behaviour observed when the aforementioned conditions are violated for the Legendre-Gauss (LG) family of operators.

2 Notation and definitions

The notation is adapted from [7,11,12,20]. Upper-case script letters, e.g., $\mathcal{U}$, denote continuous functions, while bold letters, e.g., $\boldsymbol{u}$, indicate the restriction of these continuous functions onto a set of nodes. A sans-serif capital letter, e.g., H, represents a matrix. Furthermore, $\mathbf{0} = [0,0,\ldots,0]^{\mathrm{T}}$ and $\mathbf{1} = [1,1,\ldots,1]^{\mathrm{T}}$ denote vectors of all zeros and all ones, respectively.

Let $\Omega \subset \mathbb{R}^d$ denote a d-dimensional Lipschitz domain with the boundary $\Gamma \equiv \partial\Omega$. To introduce our discretization, we decompose the physical domain, Ω, into K nonoverlapping elements Ω_κ, $\kappa = 1,\ldots,K$, such that $\overline{\Omega} = \cup_{\kappa=1}^K \overline{\Omega}_\kappa$, $\Omega_i \cap \Omega_j$, $i \neq j$, where $\overline{\Omega}_\kappa \equiv \Omega_\kappa \cup \Gamma_\kappa$ denotes the closure of Ω_κ. Here, $\Gamma_\kappa \equiv \partial\Omega_\kappa$ delineates the boundary of Ω_κ. We assume that there exists a time-invariant invertible transformation on each element, $\mathcal{T}_\kappa \colon \Omega_\kappa \to \hat{\Omega}_\kappa$, which allows us to construct SBP operators on the reference domain, $\hat{\Omega}_\kappa$, whose boundary is denoted by $\hat{\Gamma}_\kappa$. The extension to a time-varying transformation on each element would introduce increased complexity through the addition of time-dependent metric terms, however in principle this extension should be straightforward, see, for example, [35]. On a given physical element, Ω_κ, the inner product and norm are defined for two square-integrable real-valued functions, $\mathcal{U}_\kappa \in L^2(\Omega_\kappa)$ and $\mathcal{V}_\kappa \in L^2(\Omega_\kappa)$, as

$$(\mathcal{U}_\kappa, \mathcal{V}_\kappa) \equiv \int_{\Omega_\kappa} \mathcal{U}_\kappa \mathcal{V}_\kappa \, d\Omega \quad \text{and} \quad \|\mathcal{U}_\kappa\|^2 \equiv \int_{\Omega_\kappa} \mathcal{U}_\kappa^2 \, d\Omega, \tag{1}$$

respectively. Using the change of variable theorem, we can recast (1) in terms of the corresponding reference element, $\hat{\Omega}_\kappa$, as

$$\int_{\Omega_\kappa} \mathcal{U}_\kappa \mathcal{V}_\kappa \, d\Omega = \int_{\hat{\Omega}_\kappa} \mathcal{U}_\kappa \mathcal{V}_\kappa \mathcal{J}_\kappa \, d\hat{\Omega} \quad \text{and} \quad \int_{\Omega_\kappa} \mathcal{U}_\kappa^2 \, d\Omega = \int_{\hat{\Omega}_\kappa} \mathcal{U}_\kappa^2 \mathcal{J}_\kappa \, d\hat{\Omega}, \tag{2}$$

where $\mathcal{J}_\kappa$ is the Jacobian of the the inverse transformation, $(\mathcal{T}_\kappa)^{-1} \colon \hat{\Omega}_\kappa \to \Omega_\kappa$. As an example, in one spatial dimension, $\mathcal{J}_\kappa \equiv dx_\kappa/d\xi$.

To approximate, for example, $\mathcal{J}_\kappa$, we introduce the following definition of a generalized SBP operator that approximates the derivative $\partial/\partial\xi$ [11].

Definition 1 (Summation-by-parts operator for the first derivative [11]) A matrix operator, $\mathsf{D}_\xi \in \mathbb{R}^{N_\xi \times N_\xi}$, is an SBP operator that approximates the derivative $\frac{\partial}{\partial\xi}$, on the domain $\xi \in (\hat{\Omega}_\xi)_\kappa = [\alpha_\xi, \beta_\xi]$ discretized with N_ξ nodes, of degree p if

1. $\mathsf{D}_\xi \boldsymbol{\xi}^k = \mathsf{H}_\xi^{-1} \mathsf{Q}_\xi \boldsymbol{\xi}^{k-1} = k\boldsymbol{\xi}^{k-1}$, $k = 0, 1, \ldots, p$;
2. H_ξ, the norm matrix, is symmetric and positive definite; and
3. $\mathsf{Q}_\xi + \mathsf{Q}_\xi^{\mathrm{T}} = \mathsf{E}_\xi$, where $\left(\boldsymbol{\xi}^i\right)^{\mathrm{T}} \mathsf{E}_\xi \boldsymbol{\xi}^j = \beta_\xi^{i+j} - \alpha_\xi^{i+j}$, $i, j, = 0, 1, \ldots r, r \geq p$.

From Definition 1, we see that the accuracy of an SBP operator is expressed in terms of the maximum degree of monomial for which it is exact. For operators constructed according to Definition 1 on tensor-product domains, it is common to decompose E_ξ as

$$\mathsf{E}_\xi = \boldsymbol{t}_{\beta_\xi}\boldsymbol{t}_{\beta_\xi}^{\mathrm{T}} - \boldsymbol{t}_{\alpha_\xi}\boldsymbol{t}_{\alpha_\xi}^{\mathrm{T}}, \quad \text{where} \quad \boldsymbol{t}_{\alpha_\xi}^{\mathrm{T}}\boldsymbol{\xi}^k = \alpha_\xi^k, \quad \boldsymbol{t}_{\beta_\xi}^{\mathrm{T}}\boldsymbol{\xi}^k = \beta_\xi^k, \quad k = 0, 1, \dots, r.$$

Here, $\boldsymbol{t}_{\alpha_\xi}$ and $\boldsymbol{t}_{\beta_\xi}$ are examples of interpolation/extrapolation operators. In multiple dimensions, the one-dimensional operators in the other coordinate directions are defined in a similar manner and extended to multiple dimensions using the tensor product formalism. This is accomplished through the following definition of a Kronecker tensor product:

Definition 2 (Kronecker tensor product) Let $\mathsf{A} \in \mathbb{R}^{n \times m}$ and $\mathsf{B} \in \mathbb{R}^{p \times q}$. The Kronecker tensor product (or tensor product) between A and B, $\mathsf{A} \otimes \mathsf{B} \in \mathbb{R}^{np \times mq}$, is defined by

$$\mathsf{A} \otimes \mathsf{B} \equiv \begin{bmatrix} a_{11}\mathsf{B} & \dots & a_{1m}\mathsf{B} \\ \vdots & \ddots & \vdots \\ a_{n1}\mathsf{B} & \dots & a_{nm}\mathsf{B} \end{bmatrix}.$$

Following [9], to facilitate the analysis in multiple dimensions, it is helpful to recast the tensor-product operators as multidimensional SBP operators. For example, in two-dimensions, the operator in the ξ direction is defined by:

$$\begin{aligned}
\tilde{\mathsf{D}}_\xi &\equiv \tilde{\mathsf{H}}^{-1}\tilde{\mathsf{Q}}_\xi, & \tilde{\mathsf{H}} &\equiv \mathsf{H}_\xi \otimes \mathsf{H}_\eta, & \tilde{\mathsf{Q}}_\xi &\equiv \mathsf{Q}_\xi \otimes \mathsf{H}_\eta, \\
\tilde{\mathsf{E}}_\xi &\equiv \tilde{\mathsf{E}}_{\beta_\xi} + \tilde{\mathsf{E}}_{\alpha_\xi}, & \tilde{\mathsf{E}}_{\alpha_\xi} &\equiv -\tilde{\mathsf{R}}_{\alpha_\xi}^{\mathrm{T}}\tilde{\mathsf{H}}_\xi^\perp\tilde{\mathsf{R}}_{\alpha_\xi}, & \tilde{\mathsf{E}}_{\beta_\xi} &\equiv \tilde{\mathsf{R}}_{\beta_\xi}^{\mathrm{T}}\tilde{\mathsf{H}}_\xi^\perp\tilde{\mathsf{R}}_{\beta_\xi}, \\
\tilde{\mathsf{H}}_\xi^\perp &\equiv \mathsf{H}_\eta, & \tilde{\mathsf{R}}_{\alpha_\xi} &\equiv \boldsymbol{t}_{\alpha_\xi}^{\mathrm{T}} \otimes \mathsf{I}_\eta, & \tilde{\mathsf{R}}_{\beta_\xi} &\equiv \boldsymbol{t}_{\beta_\xi}^{\mathrm{T}} \otimes \mathsf{I}_\eta.
\end{aligned}$$

To interpret the meaning of the preceding matrices, let $\boldsymbol{p}_\kappa$ and $\boldsymbol{q}_\kappa$ be the restriction of the continuous functions $\mathcal{P}_\kappa \in L^2(\hat{\Omega}_\kappa)$ and $\mathcal{Q}_\kappa \in L^2(\hat{\Omega}_\kappa)$, respectively, defined over the reference domain, onto the nodes of the reference domain. Then, as an example, we can relate the continuous representation of integration-by-parts to the various preceding matrices as follows

$$\underbrace{\int_{\hat{\Omega}_\kappa} \mathcal{P}_\kappa \frac{\partial \mathcal{Q}_\kappa}{\partial \xi}\, d\hat{\Omega}}_{\wr\wr} + \underbrace{\int_{\hat{\Omega}_\kappa} \frac{\partial \mathcal{P}_\kappa}{\partial \xi} \mathcal{Q}_\kappa\, d\hat{\Omega}}_{\wr\wr} = \underbrace{\oint_{\hat{\Gamma}_\kappa} \mathcal{P}_\kappa \mathcal{Q}_\kappa n_\xi\, d\hat{\Gamma}}_{\wr\wr}$$

$$\overbrace{\boldsymbol{p}_\kappa^{\mathrm{T}}\tilde{\mathsf{H}}\tilde{\mathsf{D}}_\xi\boldsymbol{q}_\kappa} + \overbrace{\boldsymbol{p}_\kappa^{\mathrm{T}}(\tilde{\mathsf{H}}\tilde{\mathsf{D}}_\xi)^{\mathrm{T}}\boldsymbol{q}_\kappa} = \overbrace{\boldsymbol{p}_\kappa^{\mathrm{T}}\tilde{\mathsf{E}}_\xi\boldsymbol{q}_\kappa}$$

where n_ξ is the is the ξ component of the unit normal on $\hat{\Gamma}_\kappa$. Finally, we have

$$\tilde{\mathsf{R}}_{\alpha_\xi}\boldsymbol{u}_\kappa \approx \mathcal{U}_\kappa(\boldsymbol{\xi}^{\alpha_\xi}, \boldsymbol{\eta}^{\alpha_\xi}) \quad \text{and} \quad \tilde{\mathsf{R}}_{\beta_\xi}\boldsymbol{u}_\kappa \approx \mathcal{U}_\kappa(\boldsymbol{\xi}^{\beta_\xi}, \boldsymbol{\eta}^{\beta_\xi}),$$

where, as an example, $\boldsymbol{\xi}^{\alpha_\xi}$ and $\boldsymbol{\eta}^{\alpha_\xi}$ are the coordinates of the nodes at the surface $\hat{\Gamma}_\kappa^{\alpha_\xi}$, which is perpendicular to ξ.

We recognize two classes of SBP operators: classical SBP operators and generalized SBP operators [11]. Classical SBP operators are constructed with a repeated interior stencil on a uniform nodal distribution that includes both boundary nodes. Generalized SBP operators can be constructed on nonuniform nodal distributions that do not include one or both boundary nodes. A classical diagonal-norm SBP operator of degree p is associated with a degree $\tau = 2p-1$ quadrature rule, while a generalized diagonal-norm SBP operator of degree p is associated with a degree $\tau \geq 2p - 1$ quadrature rule [11]. The order of a quadrature is equal to $\tau + 1$. Note that classical SBP operators are a subset of generalized SBP operators.

Table 1 lists the generalized SBP operators that are used throughout this paper. The Legendre-Gauss-Lobatto (LGL) nodal distributions include the boundary nodes (denoted by the solid black circles ●), and therefore the interpolation/extrapolation operators associated with this class of nodal distributions are exact (i.e., $r = \infty$). The degree $p = N_\xi - 1$ Legendre-Gauss (LG) quadrature nodes, which do not include boundary nodes, are found by solving $P_{N_\xi}(\xi) = 0$, where $P_{N_\xi}(\xi)$ is the N_ξ^{th} Legendre polynomial and is given by [24]

$$P_{N_\xi}(\xi) = \frac{1}{2^{N_\xi}} \sum_{k=0}^{N_\xi} \binom{N_\xi}{k}^2 (\xi - 1)^{N_\xi - k} \xi^k \quad \forall \xi \in [0,1].$$

Similarly, the degree $p = N_\xi - 1$ LGL quadrature nodes, which do include boundary nodes, are found by solving $dP_{N_\xi - 1}(\xi)/d\xi = 0$.

We can construct the operators in Table 1 by starting with their respective nodal distributions and then solving the accuracy conditions prescribed by Definition 1; however it is easier to assemble these specific operators directly using [4,8]:

$$\mathsf{H}_\xi(i,i) = \int_{\alpha_\xi}^{\beta_\xi} \ell_i(\xi)\ell_i(\xi)\,d\xi \quad \text{and} \quad \mathsf{Q}_\xi(i,j) = \int_{\alpha_\xi}^{\beta_\xi} \ell_i(\xi)\frac{d\ell_j(\xi)}{d\xi}\,d\xi,$$

for all $(i,j) \in [1, N_\xi]$, where $\ell_i(\xi)$ denotes the ith Lagrangian basis function, given by

$$\ell_i(\xi) \equiv \prod_{\substack{1 \leq m \leq N_\xi \\ m \neq i}} \left(\frac{\xi - \xi_m}{\xi_i - \xi_m} \right).$$

As an example, taking $[\alpha_\xi, \beta_\xi] = [0,1]$, a degree-two element-type SBP operator constructed on the Legendre-Gauss quadrature nodes,

$$\boldsymbol{\xi} = \left[-\tfrac{1}{10}\sqrt{15} + \tfrac{1}{2}, \tfrac{1}{2}, \tfrac{1}{10}\sqrt{15} + \tfrac{1}{2} \right]^{\text{T}},$$

is given by

$$\mathsf{D}_\xi = \mathsf{H}_\xi^{-1}\mathsf{Q}_\xi = \begin{bmatrix} -\sqrt{15} & \frac{4}{3}\sqrt{15} & -\frac{1}{3}\sqrt{15} \\ -\frac{1}{3}\sqrt{15} & 0 & \frac{1}{3}\sqrt{15} \\ \frac{1}{3}\sqrt{15} & -\frac{4}{3}\sqrt{15} & \sqrt{15} \end{bmatrix}$$

Operator family	Nodal distribution	Operator degree, p	Interpolation/ extrapolation degree, r	Quadrature degree, τ
LGL		1	∞	$2p - 1 = 1$
LGL		2	∞	$2p - 1 = 3$
LGL		3	∞	$2p - 1 = 5$
LGL		4	∞	$2p - 1 = 7$
LG		1	1	$2p + 1 = 3$
LG		2	2	$2p + 1 = 5$
LG		3	3	$2p + 1 = 7$
LG		4	4	$2p + 1 = 9$
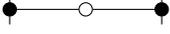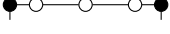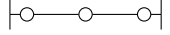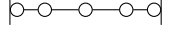
Table 1: Legendre-Gauss-Lobatto (LGL) and Legendre-Gauss (LG) generalized summation-by-parts (SBP) operators that satisfy Definition 1.

where the interpolation/extrapolation operators are constructed using Lagrangian basis functions [11] and are given by, for example,

$$\boldsymbol{t}_{\alpha_\xi} = \left[\ell_1(\alpha_\xi), \ell_2(\alpha_\xi), \ell_3(\alpha_\xi)\right]^{\mathrm{T}} = \left[\tfrac{1}{6}\sqrt{15} + \tfrac{5}{6}, -\tfrac{2}{3}, -\tfrac{1}{6}\sqrt{15} + \tfrac{5}{6}\right]^{\mathrm{T}},$$

with $\boldsymbol{t}_{\beta_\xi}$ defined in a similar manner. Details regarding a more general procedure for the construction of the operators listed in Table 1 can be found in [11].

3 The model problem

In this section we introduce the model problem that is used to exposit the main theory and generate a portion of the numerical results. The majority of the subsequent analysis in Section 4 is focused on the model problem, which is a one-dimensional boundary-value problem. Although this is a very simple problem, it provides a clear framework to present the main ideas, which are then extended to a two-dimensional boundary-value problem and the two-dimensional linear convection equation.

3.1 One-dimensional boundary-value problem

Consider the one-dimensional boundary-value problem

$$\begin{aligned}
\frac{d\mathcal{U}(x)}{dx} &= \mathcal{F}(x) \quad \forall x \in \Omega_x = [\alpha_x, \beta_x] \\
\mathcal{U}(x = \alpha_x) &= \mathcal{U}_{\mathrm{L}},
\end{aligned} \tag{3}$$

where $\mathcal{F}(x) \in L^2(\Omega_x)$ and $\mathcal{U}_{\mathrm{L}}$ is a real constant. To derive the dual problem, we recast (3) in variational form using the dual-weighted residual method as: find $\mathcal{U} \in W_{\mathrm{trial}}$ such that

$$\mathcal{R}(\mathcal{U}, \psi) \equiv \int_{\Omega_x} \psi \left(\mathcal{F}(x) - \frac{d\mathcal{U}(x)}{dx} \right) d\Omega_x - \psi(\mathcal{U} - \mathcal{U}_{\mathrm{L}})|_{x=\alpha_x}$$

$$= 0$$

for all $\psi \in W_{\mathrm{test}}$. Here, W_{trial} and W_{test} are suitable function spaces. We introduce the residual-augmented linear functional

$$\mathcal{I}(\mathcal{U}) = \int_{\Omega_x} \mathcal{G}(x)\mathcal{U}(x) \, d\Omega_x + \psi_{\mathrm{R}}(\mathcal{U}(x))|_{x=\beta_x} + \underbrace{\mathcal{R}(\mathcal{U}, \psi)}_{=0}$$

$$= \int_{\Omega_x} \psi(x)\mathcal{F}(x) \, d\Omega_x + \mathcal{U}_{\mathrm{L}}(\psi(x))|_{x=\alpha_x} + \underbrace{\mathcal{R}^*(\psi, \mathcal{U})}_{\text{dual residual}},$$

where we have used the dual residual, defined by

$$\mathcal{R}^*(\psi, \mathcal{U}) \equiv \int_{\Omega_x} \mathcal{U} \left(\mathcal{G}(x) + \frac{d\psi(x)}{dx} \right) d\Omega_x - \mathcal{U}(\psi - \psi_{\mathrm{R}})|_{x=\beta_x}.$$

Here, $\mathcal{G}(x) \in L^2(\Omega_x)$ and ψ_{R} is a real constant. In general, the dual residual, $\mathcal{R}^*(\psi, \mathcal{U})$, is nonzero; however suppose we choose ψ such that $\mathcal{R}^*(\psi, \mathcal{U}) = 0$. In this case, the strong form of the dual problem is extracted from the dual residual as

$$-\frac{d\psi(x)}{dx} = \mathcal{G}(x) \quad \forall x \in \Omega_x = [\alpha_x, \beta_x]$$

$$\psi(x = \beta_x) = \psi_{\mathrm{R}}. \tag{4}$$

Beginning in Section 4.2, we use the model problem developed herein to present the main theory, which pertains to functional superconvergence.

4 Analysis

Solving PDEs on complex geometries normally requires the use of a curvilinear coordinate transformation which relates points in the physical domain to points in a reference space. For classical diagonal-norm SBP operators, the impact that the geometric terms introduced by the coordinate transformation have on the accuracy of diagonal-norm SBP quadrature was studied in [21]. It was found that classical diagonal-norm SBP quadrature retains its order $2p$ theoretical accuracy in curvilinear coordinates when the Jacobian of the transformation is constructed using the SBP derivative operator associated with the quadrature (i.e., the norm matrix, H_ξ). For tensor-product domains, besides retaining quadrature accuracy for classical SBP operators, the motivation for constructing the metric Jacobian using the SBP derivative operator associated with the norm arises from studies by, for example, [35], that imply that the derivative operators used to approximate the fluxes should also be used to compute the metrics to satisfy the metric invariants.

4.1 Quadrature accuracy of summation-by-parts operators

To see the effect of curvilinear transformations on the quadrature accuracy of generalized SBP schemes that do not include one or both boundary nodes, we begin in a single dimension, similar to [21]. Consider mapping an integral from an element in physical space to the corresponding element in reference space. For $\mathcal{U}_\kappa \in L^2((\Omega_x)_\kappa)$, the change of variable theorem gives

$$\int_{(\Omega_x)_\kappa} \mathcal{U}_\kappa \, d\Omega_x = \int_{(\hat{\Omega}_\xi)_\kappa} \mathcal{U}_\kappa \mathcal{J}_\kappa \, d\hat{\Omega}_\xi. \tag{5}$$

Using SBP operators, we can compute

$$\mathsf{J}_\kappa = \mathrm{diag}(\mathsf{D}_\xi \boldsymbol{x}_\kappa) \approx \mathrm{diag}([\mathcal{J}_\kappa(\xi_1), \mathcal{J}_\kappa(\xi_2), \ldots, \mathcal{J}_\kappa(\xi_{N_\xi})]^\mathrm{T}) \tag{6}$$

and approximate the right-hand side of (5) as

$$\boldsymbol{u}_\kappa^\mathrm{T} \mathsf{H}_\xi \mathsf{J}_\kappa \boldsymbol{1} = \boldsymbol{u}_\kappa^\mathrm{T} \mathsf{Q}_\xi \boldsymbol{x}_\kappa \approx \int_{(\hat{\Omega}_\xi)_\kappa} \mathcal{U}_\kappa \mathcal{J}_\kappa \, d\hat{\Omega}_\xi. \tag{7}$$

Note that, throughout this work, $\mathsf{H}_\xi \mathsf{J}_\kappa = \mathsf{J}_\kappa \mathsf{H}_\xi$, since both H_ξ and J_κ are diagonal matrices. The appearance of Q_ξ in (7) motivates an investigation of the accuracy of Q_ξ.

For classical SBP operators, [21] introduces and proves the following theorem to show that (7) is a $2p$-order accurate approximation to the right-hand side of (5), where we use the notation of the present work to reproduce the theorem.

Theorem 1 *Let $\mathsf{D}_\xi = \mathsf{H}_\xi^{-1} \mathsf{Q}_\xi$ be an SBP operator of degree p approximating the first derivative. Then*

$$(\boldsymbol{z}_\kappa, \mathsf{D}_\xi \boldsymbol{u}_\kappa)_{\mathsf{H}_\xi} = \boldsymbol{z}_\kappa^\mathrm{T} \mathsf{Q}_\xi \boldsymbol{u}_\kappa$$

is a $2p$-order accurate approximation to the integral

$$\int_{(\hat{\Omega}_\xi)_\kappa} \mathcal{Z}_\kappa \frac{d\mathcal{U}_\kappa}{d\xi} \, d\hat{\Omega}_\xi,$$

where $\mathcal{Z}_\kappa \frac{d\mathcal{U}_\kappa}{d\xi} \in C^{2p-1}((\hat{\Omega}_\xi)_\kappa)$.

Proof See [21] for the proof.   □

Remark 1 The first derivative SBP operator in Theorem 1 is a classical SBP operator constructed on a uniform domain that includes both boundary nodes.

For generalized SBP operators, we can prove an analogous theorem, which is essentially the same as Theorem 3.4 in [18], where the proof is similar to that given in [21] for Theorem 1 above. The theorem and proof follow.

Theorem 2 *Let* $\mathsf{D}_\xi = \mathsf{H}_\xi^{-1}\mathsf{Q}_\xi$ *be a generalized SBP operator of degree p approximating the first derivative operator, as in Definition 1. Then*

$$(\boldsymbol{z}_\kappa, \mathsf{D}_\xi \boldsymbol{u}_\kappa)_{\mathsf{H}_\xi} = \boldsymbol{z}_\kappa^{\mathrm{T}}\mathsf{Q}_\xi \boldsymbol{u}_\kappa = \int_{(\hat{\Omega}_\xi)_\kappa} \mathcal{Z}_\kappa \frac{d\mathcal{U}_\kappa}{d\xi} \, d\hat{\Omega}_\xi, \quad i, j \leq r, i + j \leq 2p,$$

where $\mathcal{Z}_\kappa \frac{d\mathcal{U}_\kappa}{d\xi} \in C^{2p-1}((\hat{\Omega}_\xi)_\kappa)$, $\boldsymbol{z}_\kappa = \boldsymbol{\xi}^i$, and $\boldsymbol{u}_\kappa = \boldsymbol{\xi}^j$.

Proof Let $\boldsymbol{u}_\kappa'$ and $\boldsymbol{z}_\kappa'$ be the exact derivatives of $\mathcal{U}_\kappa$ and $\mathcal{Z}_\kappa$ evaluated at the element nodes, respectively. Due to the accuracy of H_ξ, the result will follow if we can show that

$$(\boldsymbol{z}_\kappa, \boldsymbol{u}_\kappa')_{\mathsf{H}_\xi} = (\boldsymbol{z}, \mathsf{D}_\xi \boldsymbol{u}_\kappa)_{\mathsf{H}_\xi}, \quad i, j \leq r, i + j \leq 2p. \tag{8}$$

First take $j \leq p$, this gives

$$\mathsf{D}_\xi \boldsymbol{u}_\kappa = j\boldsymbol{\xi}^{j-1} = \boldsymbol{u}_\kappa', \tag{9}$$

which means $(\boldsymbol{z}_\kappa, \boldsymbol{u}_\kappa')_{\mathsf{H}_\xi} = (\boldsymbol{z}_\kappa, \mathsf{D}_\xi \boldsymbol{u}_\kappa)_{\mathsf{H}_\xi}$ for $j \leq p$. Next, we consider $j \geq p$, which means that $i \leq p$ and $\mathsf{D}_\xi \boldsymbol{z}_\kappa = i\boldsymbol{\xi}^{i-1} = \boldsymbol{z}_\kappa'$. Using $\mathsf{D}_\xi \boldsymbol{z}_\kappa = \boldsymbol{z}_\kappa'$ along with the SBP property, $\mathsf{Q}_\xi + \mathsf{Q}_\xi^{\mathrm{T}} = \mathsf{E}_\xi$, gives

$$\begin{aligned}
(\boldsymbol{z}_\kappa, \mathsf{D}_\xi \boldsymbol{u}_\kappa)_{\mathsf{H}_\xi} &= \boldsymbol{z}_\kappa^{\mathrm{T}}\mathsf{H}_\xi \mathsf{D}_\xi \boldsymbol{u}_\kappa \\
&= \boldsymbol{z}_\kappa^{\mathrm{T}}(\mathsf{E}_\xi - \mathsf{Q}_\xi^{\mathrm{T}})\boldsymbol{u}_\kappa \\
&= \boldsymbol{z}_\kappa^{\mathrm{T}}\mathsf{E}_\xi \boldsymbol{u}_\kappa - \boldsymbol{z}_\kappa^{\mathrm{T}}\mathsf{Q}_\xi^{\mathrm{T}}\boldsymbol{u}_\kappa \\
&= \boldsymbol{z}_\kappa^{\mathrm{T}}\mathsf{E}_\xi \boldsymbol{u}_\kappa - (\boldsymbol{u}_\kappa, \mathsf{D}_\xi \boldsymbol{z}_\kappa)_{\mathsf{H}_\xi} \\
&= \boldsymbol{z}_\kappa^{\mathrm{T}}\mathsf{E}_\xi \boldsymbol{u}_\kappa - (\boldsymbol{u}_\kappa, \boldsymbol{z}_\kappa')_{\mathsf{H}_\xi} \\
&= \boldsymbol{z}_\kappa^{\mathrm{T}}\mathsf{E}_\xi \boldsymbol{u}_\kappa - \int_{(\hat{\Omega}_\xi)_\kappa} \mathcal{U}_\kappa \frac{d\mathcal{Z}_\kappa}{d\xi} \, d\hat{\Omega}_\xi,
\end{aligned}$$

or, taking $i, j \leq r$ and using the accuracy condition on E_ξ gives,

$$\begin{aligned}
(\boldsymbol{z}_\kappa, \mathsf{D}_\xi \boldsymbol{u}_\kappa)_{\mathsf{H}_\xi} &= \boldsymbol{z}_\kappa^{\mathrm{T}}\mathsf{E}_\xi \boldsymbol{u}_\kappa - \int_{(\hat{\Omega}_\xi)_\kappa} \mathcal{U}_\kappa \frac{d\mathcal{Z}_\kappa}{d\xi} \, d\hat{\Omega}_\xi \\
&= \int_{(\hat{\Omega}_\xi)_\kappa} \frac{d(\mathcal{U}_\kappa \mathcal{Z}_\kappa)}{d\xi} \, d\hat{\Omega}_\xi - \int_{(\hat{\Omega}_\xi)_\kappa} \mathcal{U}_\kappa \frac{d\mathcal{Z}_\kappa}{d\xi} \, d\hat{\Omega}_\xi \\
&= \int_{(\hat{\Omega}_\xi)_\kappa} \mathcal{Z}_\kappa \frac{d\mathcal{U}_\kappa}{d\xi} \, d\hat{\Omega}_\xi.
\end{aligned}$$

Therefore, $(\boldsymbol{z}_\kappa, \boldsymbol{u}_\kappa')_{\mathsf{H}_\xi} = (\boldsymbol{z}_\kappa, \mathsf{D}_\xi \boldsymbol{u})_{\mathsf{H}_\xi}$ for $j \geq p$ and $i, j \leq r$, with $i + j \leq 2p$. We have thus shown the desired result. $\qquad\square$

From Theorems 1 and 2, we can see that, for generalized SBP operators, $\boldsymbol{z}_\kappa^{\mathrm{T}}\mathsf{Q}_\xi \boldsymbol{u}_\kappa$ is at least a $2p$-order approximation of $\int_{(\hat{\Omega}_\xi)_\kappa} \mathcal{Z}_\kappa \frac{d\mathcal{U}_\kappa}{d\xi} \, d\hat{\Omega}_\xi$ if and only if $r \geq 2p$. This is a more stringent condition compared to Definition 1 where the accuracy requirement on r is $r \geq p$. The implication of Theorem 2 is

that quadrature accuracy in curvilinear coordinates is decreased for generalized SBP operators if: (1) $r < 2p$, (2) the Jacobian of the transformation is approximated by the same SBP operator that is associated with the norm, and (3) an element uses a higher degree representation of the geometry compared to the degree of the SBP operator associated with that element.

4.2 Functional superconvergence

The practical implication of this theoretical decrease in quadrature accuracy under the preceding conditions is the loss of superconvergent functionals in curvilinear coordinates under the above conditions. To appreciate this, we take a small detour and examine functional superconvergence for tensor-product generalized SBP operators in curvilinear coordinates in a one-dimensional setting that extends to multiple dimensions through tensor products. We build upon [20], which explains functional superconvergence for tensor-product classical SBP discretizations, and [2,3], which extend the theory of superconvergent linear functionals to generalized SBP time-marching methods.

Our initial aim is to discretize the model problem introduced in Section 3. To proceed with our discretization, we tessellate the full domain into elements and map each element to the reference domain, as described in Section 2. On the κth element, (3) becomes

$$\mathcal{J}_\kappa^{-1} \frac{d\mathcal{U}_\kappa(\xi)}{d\xi} = \mathcal{F}_\kappa(\xi) \quad \forall \xi \in (\hat{\Omega}_\xi)_\kappa = [\alpha_\xi, \beta_\xi]$$
$$\mathcal{U}_\kappa(\xi = \alpha_\xi) = (\mathcal{U}_{\text{L}})_\kappa. \tag{10}$$

The associated discretization on the κth element is given by

$$\mathsf{J}_\kappa^{-1} \mathsf{D}_\xi (\boldsymbol{u}_h)_\kappa = \boldsymbol{f}_\kappa - \overbrace{\mathsf{J}_\kappa^{-1} \mathsf{H}_\xi^{-1} \boldsymbol{t}_{\alpha_\xi} (\boldsymbol{t}_{\alpha_\xi}^{\text{T}} (\boldsymbol{u}_h)_\kappa - (\mathcal{U}_{\text{L}})_\kappa)}^{\text{upwind SAT}}, \tag{11}$$

where $\boldsymbol{f}_\kappa = [\mathcal{F}_\kappa(\xi_1), \mathcal{F}_\kappa(\xi_2), \ldots, \mathcal{F}_\kappa(\xi_{N_\xi})]^{\text{T}}$, $(\mathcal{U}_{\text{L}})_1 = \mathcal{U}_{\text{L}}$, and $(\mathcal{U}_{\text{L}})_\kappa = \boldsymbol{t}_{\beta_\xi}^{\text{T}} (\boldsymbol{u}_h)_{\kappa-1}$ for $\kappa = 2, 3, \ldots, K$. We note that although (11) represents the SBP discretization of a simple problem, several examples of SBP discretizations of more general problems exist in the literature, for example, [19,30]. Also, through the mapping, our continuous and discrete functionals become

$$\mathcal{I}(\mathcal{U}) = \sum_{\kappa=1}^{K} \left(\int_{(\hat{\Omega}_\xi)_\kappa} \mathcal{G}_\kappa \mathcal{U}_\kappa \mathcal{J}_\kappa \, d\hat{\Omega}_\xi \right) + \psi_{\text{R}}(\mathcal{U}_K)|_{\xi = \beta_\xi} \tag{12}$$

and

$$\mathcal{I}_h(\boldsymbol{u}_h) = \sum_{\kappa=1}^{K} \left(\boldsymbol{g}_\kappa^{\text{T}} \mathsf{H}_\xi \mathsf{J}_\kappa (\boldsymbol{u}_h)_\kappa \right) + \psi_{\text{R}} \boldsymbol{t}_{\beta_\xi}^{\text{T}} (\boldsymbol{u}_h)_K, \tag{13}$$

respectively, where, analogous to $\boldsymbol{f}_\kappa$, $\boldsymbol{g}_\kappa = [\mathcal{G}_\kappa(\xi_1), \mathcal{G}_\kappa(\xi_2), \ldots, \mathcal{G}_\kappa(\xi_{N_\xi})]^{\text{T}}$. Note that the volume contribution to our functional is defined over the entire physical domain, which is why, after the mapping procedure, we sum over all K

elements. However, the boundary contribution to (13) only comes from element K.

Following [17], we introduce the following assumption.

Assumption 1 *The discretization (11) has a unique numerical solution, $\boldsymbol{u}_h$, that exists and whose error may be represented by $\|\boldsymbol{u} - \boldsymbol{u}_h\|_{L^\infty} = \mathcal{O}(h^{p+1})$ as $h \to 0$.*

Note that it may be possible to avoid Assumption 1 if we could show that the time-dependent problem associated with (11) is stable [29,31]. However, this would involve a skew-symmetric formulation of the model problem and here we focus on the divergence form as this form is routinely used to solve practical aerodynamics problems.

We are ultimately interested in how well $\mathcal{I}_h(\boldsymbol{u}_h)$ approximates $\mathcal{I}(\mathcal{U})$. To answer this question we introduce the following assumption and lemmas.

Assumption 2 *On each element in the physical domain $\Omega_\kappa \subset \Omega$, $\kappa = 1, \ldots K$, the mapping $\mathcal{T}_\kappa \colon \Omega_\kappa \to \hat{\Omega}_\kappa$ represents a bijective polynomial mapping of at most degree p.*

Remark 2 We can relax Assumption 2 to include higher degree polynomial mappings and nonpolynomial mappings and the subsequent theory will still hold if the degree of the associated interpolation/extrapolation operators is greater than or equal to $2p$. In general, for the regularity of the mapping, we require only C^0 continuity at element interfaces, as a result of the use of SATs. Alternatively, within each element, the mapping should have at least C^p continuity, where p is the degree of the SBP operator being used. This is because SBP operators are related to Taylor series expansions, truncated after a certain number of terms, where the number of terms kept is related to the degree of the operator under consideration. Therefore, all the derivatives in the expansion must exist up to the point where the Taylor series is truncated.

Remark 3 In practice, bijective polynomial mappings local to each element can be constructed using B-splines. See, for example, [9].

Lemma 1 *For element K, using Assumption 2, the term $\boldsymbol{t}_{\beta_\xi}^{\mathrm{T}}(\boldsymbol{u}_h)_K$ is a degree τ and order $\tau + 1$ approximation of $(\mathcal{U}_K)|_{\xi=\beta_\xi}$, where $\mathcal{U}_\kappa \in C^{\tau+1}((\hat{\Omega}_\xi)_K)$.*

Proof We have

$$(\mathcal{U}_K)|_{\xi=\beta_\xi} - \boldsymbol{t}_{\beta_\xi}^{\mathrm{T}}(\boldsymbol{u}_h)_K = \int_{(\hat{\Omega}_\xi)_K} \frac{d\mathcal{U}_K}{d\xi}\, d\hat{\Omega}_\xi + (\mathcal{U}_K)|_{\xi=\alpha_\xi} - \boldsymbol{t}_{\beta_\xi}^{\mathrm{T}}(\boldsymbol{u}_h)_K$$

$$= \int_{(\hat{\Omega}_\xi)_K} \mathcal{J}_K \mathcal{F}_K\, d\hat{\Omega}_\xi + (\mathcal{U}_{\mathrm{L}})_K - \boldsymbol{t}_{\beta_\xi}^{\mathrm{T}}(\boldsymbol{u}_h)_K$$

$$= \mathbf{1}^{\mathrm{T}}\mathsf{H}_\xi \mathsf{J}_K \boldsymbol{f}_K + \mathbf{1}^{\mathrm{T}}\boldsymbol{t}_{\alpha_\xi}(\mathcal{U}_{\mathrm{L}})_K - \boldsymbol{t}_{\beta_\xi}^{\mathrm{T}}(\boldsymbol{u}_h)_K + \mathcal{O}(h^{\tau+1}),$$

since $\mathbf{1}^{\mathrm{T}}\boldsymbol{t}_{\alpha_\xi} = 1$ and, using Assumption 2 and the accuracy of H_ξ,

$$\mathbf{1}^{\mathrm{T}}\mathsf{H}_\xi \mathsf{J}_K \boldsymbol{f}_K = \int_{(\hat{\Omega}_\xi)_K} \mathcal{J}_K \mathcal{F}_K\, d\hat{\Omega}_\xi + \mathcal{O}(h^{\tau+1}).$$

Also, from the definition of the discretization of the PDE we have

$$\mathsf{H}_\xi \mathsf{J}_K \boldsymbol{f}_K + \boldsymbol{t}_{\alpha_\xi}(\mathcal{U}_\mathrm{L})_K = (\mathsf{Q}_\xi + \boldsymbol{t}_{\alpha_\xi}\boldsymbol{t}_{\alpha_\xi}^\mathrm{T})(\boldsymbol{u}_h)_K$$

and using the summation-by-parts (SBP) property gives

$$\mathsf{H}_\xi \mathsf{J}_K \boldsymbol{f}_K + \boldsymbol{t}_{\alpha_\xi}(\mathcal{U}_\mathrm{L})_K = (-\mathsf{Q}_\xi^\mathrm{T} + \boldsymbol{t}_{\beta_\xi}\boldsymbol{t}_{\beta_\xi}^\mathrm{T})(\boldsymbol{u}_h)_K.$$

Therefore,

$$
\begin{aligned}
(\mathcal{U}_K)|_{\xi=\beta_\xi} - \boldsymbol{t}_{\beta_\xi}^\mathrm{T}(\boldsymbol{u}_h)_K &= \mathbf{1}^\mathrm{T}(\mathsf{H}_\xi \mathsf{J}_K \boldsymbol{f}_K + \boldsymbol{t}_{\alpha_\xi}(\mathcal{U}_\mathrm{L})_K) - \boldsymbol{t}_{\beta_\xi}^\mathrm{T}(\boldsymbol{u}_h)_K + \mathcal{O}(h^{\tau+1}) \\
&= \mathbf{1}^\mathrm{T}(\mathsf{Q}_\xi + \boldsymbol{t}_{\alpha_\xi}\boldsymbol{t}_{\alpha_\xi}^\mathrm{T})(\boldsymbol{u}_h)_K - \boldsymbol{t}_{\beta_\xi}^\mathrm{T}(\boldsymbol{u}_h)_K + \mathcal{O}(h^{\tau+1}) \\
&= \mathbf{1}^\mathrm{T}(-\mathsf{Q}_\xi^\mathrm{T} + \boldsymbol{t}_{\beta_\xi}\boldsymbol{t}_{\beta_\xi}^\mathrm{T})(\boldsymbol{u}_h)_K - \boldsymbol{t}_{\beta_\xi}^\mathrm{T}(\boldsymbol{u}_h)_K + \mathcal{O}(h^{\tau+1}),
\end{aligned}
$$

or, since $\mathbf{1}^\mathrm{T}\boldsymbol{t}_{\beta_\xi} = 1$ and $\mathsf{Q}_\xi \mathbf{1} = \mathbf{0}$ by construction,

$$(\mathcal{U}_K)|_{\xi=\beta_\xi} - \boldsymbol{t}_{\beta_\xi}^\mathrm{T}(\boldsymbol{u}_h)_K = \mathcal{O}(h^{\tau+1}).$$

This concludes the proof. $\qquad\square$

Remark 4 Lemma 1 is a variant of Theorem 3.4 in [3] extended to curvilinear coordinates.

Lemma 2 *For each element $\kappa = 1, 2, \ldots, K$, using Assumption 2, the term $\boldsymbol{t}_{\beta_\xi}^\mathrm{T}(\boldsymbol{u}_h)_\kappa$ is a degree τ and order $\tau + 1$ approximation of $(\mathcal{U}_k)|_{\xi=\beta_\xi}$, where $\mathcal{U}_\kappa \in C^{\tau+1}((\hat{\Omega}_\xi)_\kappa)$.*

Proof This follows immediately by considering the proof of Lemma 1 for the κth element. $\qquad\square$

Remark 5 Lemma 2 is consistent with [3], which, in the context of generalized SBP time-marching schemes, shows that the interpolation/extrapolation of the solution to the end of each time step is superconvergent.

Remark 6 The superconvergence described by Lemma 2 is consistent with the outflow superconvergence described by and exploited in, e.g., [26].

Lemma 3 *Suppose we have $\psi_\kappa \subset \psi$ and $\mathcal{U}_\kappa \subset \mathcal{U}$ such that $\psi_\kappa \frac{d\mathcal{U}_\kappa}{d\xi} \in C^{\min(2p,\tau)}$, where ψ and $\mathcal{U}$ are the dual and primal solutions, respectively, associated with the PDE and functional defined by (3) and (4), respectively. Then*

$$\boldsymbol{\psi}_\kappa^\mathrm{T}\mathsf{H}_\xi(\mathsf{D}_\xi \boldsymbol{u}_\kappa + \mathsf{H}_\xi^{-1}\boldsymbol{t}_{\alpha_\xi}(\boldsymbol{t}_{\alpha_\xi}^\mathrm{T}\boldsymbol{u}_\kappa - (\mathcal{U}_\mathrm{L})_\kappa)) - (\psi_\mathrm{R})_\kappa\boldsymbol{t}_{\beta_\xi}^\mathrm{T}\boldsymbol{u}_\kappa + (\psi_\mathrm{R})_\kappa(\mathcal{U}_\mathrm{R})_\kappa$$

is a degree $\min(2p,\tau)$ and order $\min(2p+1, \tau+1)$ approximation of

$$\int_{(\hat{\Omega}_\xi)_\kappa} \psi_\kappa \frac{d\mathcal{U}_\kappa}{d\xi}\, d\hat{\Omega}_\xi,$$

i.e.,

$$\boldsymbol{\psi}_\kappa^{\mathrm{T}} \mathsf{H}_\xi (\mathsf{D}_\xi \boldsymbol{u}_\kappa + \mathsf{H}_\xi^{-1} \boldsymbol{t}_{\alpha_\xi}(\boldsymbol{t}_{\alpha_\xi}^{\mathrm{T}} \boldsymbol{u}_\kappa - (\mathcal{U}_{\mathrm{L}})_\kappa)) - (\psi_{\mathrm{R}})_\kappa \boldsymbol{t}_{\beta_\xi}^{\mathrm{T}} \boldsymbol{u}_\kappa + (\psi_{\mathrm{R}})_\kappa (\mathcal{U}_{\mathrm{R}})_\kappa =$$
$$\int_{(\hat{\Omega}_\xi)_\kappa} \psi_\kappa \frac{d\mathcal{U}_\kappa}{d\xi} \, d\hat{\Omega}_\xi + \mathcal{O}(h^{\min(2p+1,\tau+1)}).$$

Proof We approach this proof in the same manner as the proof of Theorem 2. From the accuracy of H_ξ we have

$$\int_{(\hat{\Omega}_\xi)_\kappa} \psi_\kappa \frac{d\mathcal{U}_\kappa}{d\xi} \, \hat{\Omega}_\xi = (\boldsymbol{\psi}_\kappa, \boldsymbol{u}_\kappa')_{\mathsf{H}_\xi} + \mathcal{O}(h^{\tau+1}).$$

Here, $\boldsymbol{u}_\kappa'$ is $\frac{d\mathcal{U}_\kappa}{d\xi}$ at the nodes. Based on the accuracy of H_ξ, we would like to show

$$(\boldsymbol{\psi}_\kappa, \boldsymbol{u}_\kappa')_{\mathsf{H}_\xi} = \boldsymbol{\psi}_\kappa^{\mathrm{T}} \mathsf{H}_\xi (\mathsf{D}_\xi \boldsymbol{u}_\kappa + \mathsf{H}_\xi^{-1} \boldsymbol{t}_{\alpha_\xi}(\boldsymbol{t}_{\alpha_\xi}^{\mathrm{T}} \boldsymbol{u}_\kappa - (\mathcal{U}_{\mathrm{L}})_\kappa))$$
$$- (\psi_{\mathrm{R}})_\kappa \boldsymbol{t}_{\beta_\xi}^{\mathrm{T}} \boldsymbol{u}_\kappa + (\psi_{\mathrm{R}})_\kappa (\mathcal{U}_{\mathrm{R}})_\kappa + \mathcal{O}(h^{\min(2p+1,\tau+1)}).$$

Using a similar argument as in [21], it is sufficient to show that the preceding equation is exact for polynomial integrands of degree less than $2p+1$. To this end, we consider $\boldsymbol{\psi}_\kappa = \boldsymbol{p}_k$ and $\boldsymbol{u}_\kappa = \boldsymbol{p}_m$ as degree k and m polynomials, respectively, where $k + m \le 2p + 1$ defines the highest permissible degree of the combined integrand. We begin by taking $m \le p$, which gives

$$\boldsymbol{\psi}_\kappa^{\mathrm{T}} \mathsf{H}_\xi (\mathsf{D}_\xi \boldsymbol{u}_\kappa + \mathsf{H}_\xi^{-1} \boldsymbol{t}_{\alpha_\xi}(\boldsymbol{t}_{\alpha_\xi}^{\mathrm{T}} \boldsymbol{u}_\kappa - (\mathcal{U}_{\mathrm{L}})_\kappa)) - (\psi_{\mathrm{R}})_\kappa \boldsymbol{t}_{\beta_\xi}^{\mathrm{T}} \boldsymbol{u}_\kappa + (\psi_{\mathrm{R}})_\kappa (\mathcal{U}_{\mathrm{R}})_\kappa = \boldsymbol{\psi}_\kappa^{\mathrm{T}} \mathsf{H}_\xi \boldsymbol{u}_\kappa'$$
$$= (\boldsymbol{\psi}_\kappa, \boldsymbol{u}_\kappa')_{\mathsf{H}_\xi}.$$

Next, we reverse the situation and take $m > p$, which means we must have $k < p + 1$ due to the condition that $k + m \le 2p + 1$. For this case we have

$$\boldsymbol{\psi}_\kappa^{\mathrm{T}} \mathsf{H}_\xi (\mathsf{D}_\xi \boldsymbol{u}_\kappa + \mathsf{H}_\xi^{-1} \boldsymbol{t}_{\alpha_\xi}(\boldsymbol{t}_{\alpha_\xi}^{\mathrm{T}} \boldsymbol{u}_\kappa - (\mathcal{U}_{\mathrm{L}})_\kappa)) - (\psi_{\mathrm{R}})_\kappa \boldsymbol{t}_{\beta_\xi}^{\mathrm{T}} \boldsymbol{u}_\kappa + (\psi_{\mathrm{R}})_\kappa (\mathcal{U}_{\mathrm{R}})_\kappa$$
$$= \boldsymbol{\psi}_\kappa^{\mathrm{T}} (\mathsf{E}_\xi - \mathsf{Q}_\xi^{\mathrm{T}}) \boldsymbol{u}_\kappa + \boldsymbol{\psi}_\kappa^{\mathrm{T}} \boldsymbol{t}_{\alpha_\xi}(\boldsymbol{t}_{\alpha_\xi}^{\mathrm{T}} \boldsymbol{u}_\kappa - (\mathcal{U}_{\mathrm{L}})_\kappa) - (\psi_{\mathrm{R}})_\kappa \boldsymbol{t}_{\beta_\xi}^{\mathrm{T}} \boldsymbol{u}_\kappa + (\psi_{\mathrm{R}})_\kappa (\mathcal{U}_{\mathrm{R}})_\kappa$$
$$= \boldsymbol{\psi}_\kappa^{\mathrm{T}} (\boldsymbol{t}_{\beta_\xi} \boldsymbol{t}_{\beta_\xi}^{\mathrm{T}} - \mathsf{Q}_\xi^{\mathrm{T}}) \boldsymbol{u}_\kappa - \boldsymbol{\psi}_\kappa^{\mathrm{T}} \boldsymbol{t}_{\alpha_\xi}(\mathcal{U}_{\mathrm{L}})_\kappa - (\psi_{\mathrm{R}})_\kappa \boldsymbol{t}_{\beta_\xi}^{\mathrm{T}} \boldsymbol{u}_\kappa + (\psi_{\mathrm{R}})_\kappa (\mathcal{U}_{\mathrm{R}})_\kappa$$
$$= \underline{(\psi_{\mathrm{R}})_\kappa \boldsymbol{t}_{\beta_\xi}^{\mathrm{T}} \boldsymbol{u}_\kappa} - \boldsymbol{\psi}_\kappa^{\mathrm{T}} \mathsf{Q}_\xi^{\mathrm{T}} \boldsymbol{u}_\kappa - (\psi_{\mathrm{L}})_\kappa (\mathcal{U}_{\mathrm{L}})_\kappa - \underline{(\psi_{\mathrm{R}})_\kappa \boldsymbol{t}_{\beta_\xi}^{\mathrm{T}} \boldsymbol{u}_\kappa} + (\psi_{\mathrm{R}})_\kappa (\mathcal{U}_{\mathrm{R}})_\kappa$$
$$= -(\mathsf{D}_\xi \boldsymbol{\psi}_\kappa)^{\mathrm{T}} \mathsf{H}_\xi \boldsymbol{u}_\kappa + (\psi_{\mathrm{R}})_\kappa (\mathcal{U}_{\mathrm{R}})_\kappa - (\psi_{\mathrm{L}})_\kappa (\mathcal{U}_{\mathrm{L}})_\kappa$$
$$= -(\boldsymbol{\psi}_\kappa')^{\mathrm{T}} \mathsf{H}_\xi \boldsymbol{u}_\kappa + (\psi_\kappa \mathcal{U}_\kappa)|_{\xi=\alpha_\xi}^{\xi=\beta_\xi}$$
$$= -\int_{(\hat{\Omega}_\xi)_\kappa} \frac{d\psi_\kappa}{d\xi} \mathcal{U}_\kappa \, d\hat{\Omega}_\xi + (\psi_\kappa \mathcal{U}_\kappa)|_{\xi=\alpha_\xi}^{\xi=\beta_\xi} + \mathcal{O}(h^{\tau+1})$$
$$= \int_{(\hat{\Omega}_\xi)_\kappa} \psi_\kappa \frac{d\mathcal{U}_\kappa}{d\xi} \, dx + \mathcal{O}(h^{\tau+1}).$$

Since $k + m \le 2p + 1$, we see that $\boldsymbol{\psi}_\kappa^{\mathrm{T}} \mathsf{H}_\xi (\mathsf{D}_\xi \boldsymbol{u}_\kappa + \mathsf{H}_\xi^{-1} \boldsymbol{t}_{\alpha_\xi}(\boldsymbol{t}_{\alpha_\xi}^{\mathrm{T}} \boldsymbol{u}_\kappa - (\mathcal{U}_{\mathrm{L}})_\kappa)) - (\psi_{\mathrm{R}})_\kappa \boldsymbol{t}_{\beta_\xi}^{\mathrm{T}} \boldsymbol{u}_\kappa + (\psi_{\mathrm{R}})_\kappa (\mathcal{U}_{\mathrm{R}})_\kappa$ is an order $\min(2p + 1, \tau + 1)$ approximation of $\int_{(\hat{\Omega}_\xi)_\kappa} \psi_\kappa \frac{d\mathcal{U}_\kappa}{d\xi} \, d\hat{\Omega}_\xi$, which concludes the proof. $\square$

Remark 7 Lemma 3 is similar to Lemma 12 in [2], however here we consider general inhomogeneous $(\psi_{\mathrm{R}})_\kappa$ rather than homogeneous $(\psi_{\mathrm{R}})_\kappa = 0$.

We now return to our initial question regarding the accuracy of $\mathcal{I}_h(\boldsymbol{u}_h)$ relative to $\mathcal{I}(\mathcal{U})$ and state the following theorem as an answer.

Theorem 3 *Let $(\boldsymbol{u}_h)_\kappa \subset \boldsymbol{u}_h$ be the discrete solution that satisfies (11) for $\kappa = 1, 2, \ldots, K$. Furthermore, assume that $\mathcal{G}_\kappa \in C^{\min(2p+1,\tau+1)}((\hat{\Omega}_\xi)_\kappa)$ and $\mathcal{U}_\kappa \in C^{\min(2p+1,\tau+1)}((\hat{\Omega}_\xi)_\kappa)$. Then, using Assumption 2, $\mathcal{I}_h(\boldsymbol{u}_h)$, defined by (13),*

$$\mathcal{I}_h(\boldsymbol{u}_h) = \sum_{\kappa=1}^{K} \left(\boldsymbol{g}_\kappa^{\mathrm{T}} \mathsf{H}_\xi \mathsf{J}_\kappa (\boldsymbol{u}_h)_\kappa \right) + \psi_{\mathrm{R}} \boldsymbol{t}_{\beta_\xi}^{\mathrm{T}}(\boldsymbol{u}_h)_K,$$

is a degree $\min(2p, \tau)$ and order $\min(2p + 1, \tau + 1)$ approximation of $\mathcal{I}(\mathcal{U})$, defined by (12),

$$\mathcal{I}(\mathcal{U}) = \sum_{\kappa=1}^{K} \left(\int_{(\hat{\Omega}_\xi)_\kappa} \mathcal{G}_\kappa \mathcal{U}_\kappa \mathcal{J}_\kappa \, d\hat{\Omega}_\xi \right) + \psi_{\mathrm{R}}(\mathcal{U}_K)|_{\xi=\beta_\xi}.$$

Proof Subtracting (13) from (12) gives

$$\mathcal{I}(\mathcal{U}) - \mathcal{I}_h(\boldsymbol{u}_h)$$
$$= \sum_{\kappa=1}^{K} \left(\int_{(\hat{\Omega}_\xi)_\kappa} \mathcal{G}_\kappa \mathcal{U}_\kappa \mathcal{J}_\kappa \, d\hat{\Omega}_\xi - \boldsymbol{g}_\kappa^{\mathrm{T}} \mathsf{H}_\xi \mathsf{J}_\kappa (\boldsymbol{u}_h)_\kappa \right) + \psi_{\mathrm{R}} \left((\mathcal{U}_K)|_{\xi=\beta_\xi} - \boldsymbol{t}_{\beta_\xi}^{\mathrm{T}}(\boldsymbol{u}_h)_K \right).$$
$$(14)$$

Next, consider the contribution to the functional from the boundary portion. This portion is only affected by element K.

$$\psi_{\mathrm{R}}(\mathcal{U}_K)|_{\xi=\beta_\xi} - \psi_{\mathrm{R}} \boldsymbol{t}_{\beta_\xi}^{\mathrm{T}}(\boldsymbol{u}_h)_K = \psi_{\mathrm{R}}((\mathcal{U}_K)|_{\xi=\beta_\xi} - \boldsymbol{t}_{\beta_\xi}^{\mathrm{T}}(\boldsymbol{u}_h)_K)$$
$$= \mathcal{O}(h^{\tau+1}). \qquad \text{(using Lemma 1)}$$

Therefore,

$$\psi_{\mathrm{R}} \left((\mathcal{U}_K)|_{\xi=\beta_\xi} - \boldsymbol{t}_{\beta_\xi}^{\mathrm{T}}(\boldsymbol{u}_h)_K \right) = \mathcal{O}(h^{\tau+1}). \qquad (15)$$

Next, consider the volume contribution to the functional from the κth element.

$$\int_{(\hat{\Omega}_\xi)_\kappa} \mathcal{G}_\kappa \mathcal{U}_\kappa \mathcal{J}_\kappa \, d\hat{\Omega}_\xi - \boldsymbol{g}_\kappa^{\mathrm{T}} \mathsf{H}_\xi \mathsf{J}_\kappa (\boldsymbol{u}_h)_\kappa = \boldsymbol{g}_\kappa^{\mathrm{T}} \mathsf{H}_\xi \mathsf{J}_\kappa \boldsymbol{u}_\kappa - \boldsymbol{g}_\kappa^{\mathrm{T}} \mathsf{H}_\xi \mathsf{J}_\kappa (\boldsymbol{u}_h)_\kappa + \mathcal{O}(h^{\tau+1})$$
$$= \boldsymbol{g}_\kappa^{\mathrm{T}} \mathsf{H}_\xi \mathsf{J}_\kappa (\boldsymbol{u}_\kappa - (\boldsymbol{u}_h)_\kappa) + \mathcal{O}(h^{\tau+1})$$

Next, we must determine the order of the term $\boldsymbol{g}_\kappa^{\mathrm{T}} \mathsf{H}_\xi \mathsf{J}_\kappa (\boldsymbol{u}_\kappa - (\boldsymbol{u}_h)_\kappa)$. To do this, we first note that the discretization of the dual problem associated with the primal PDE is

$$-\mathsf{J}_\kappa^{-1} \mathsf{D}_\xi (\boldsymbol{\psi}_h)_\kappa = \boldsymbol{g}_\kappa - \mathsf{J}_\kappa^{-1} \mathsf{H}_\xi^{-1} \boldsymbol{t}_{\beta_\xi} (\boldsymbol{t}_{\beta_\xi}^{\mathrm{T}}(\boldsymbol{\psi}_h)_\kappa - (\psi_{\mathrm{R}})_\kappa). \qquad (16)$$

Note that we can restate Assumption 1 for the dual problem.

Assumption 3 *The discretization (16) has a unique numerical solution, $\boldsymbol{\psi}_h$, that exists and whose error may be represented by $\|\boldsymbol{\psi} - \boldsymbol{\psi}_h\|_{L^\infty} = \mathcal{O}(h^{p+1})$ as $h \to 0$.*

Based on our PDEs, we can define the truncation error associated with the primal and dual problems, respectively, as

$$\boldsymbol{e}_{\mathcal{U}_\kappa} = \mathsf{J}_\kappa^{-1}\mathsf{D}_\xi \boldsymbol{u}_\kappa - \boldsymbol{f}_\kappa + \mathsf{J}_\kappa^{-1}\mathsf{H}_\xi^{-1}\boldsymbol{t}_{\alpha_\xi}(\boldsymbol{t}_{\alpha_\xi}^{\mathrm{T}}\boldsymbol{u}_\kappa - (\mathcal{U}_{\mathrm{L}})_\kappa)$$

$$\boldsymbol{e}_{\psi_\kappa} = -\mathsf{J}_\kappa^{-1}\mathsf{D}_\xi \boldsymbol{\psi}_\kappa - \boldsymbol{g}_\kappa + \mathsf{J}_\kappa^{-1}\mathsf{H}_\xi^{-1}\boldsymbol{t}_{\beta_\xi}(\boldsymbol{t}_{\beta_\xi}^{\mathrm{T}}\boldsymbol{\psi}_\kappa - (\psi_{\mathrm{R}})_\kappa).$$

Multiplying $\boldsymbol{e}_{\mathcal{U}_\kappa}$ by $\mathsf{H}_\xi \mathsf{J}_\kappa$ and rearranging gives

$$\mathsf{H}_\xi \mathsf{J}_\kappa \boldsymbol{e}_{\mathcal{U}_\kappa} - (\mathsf{Q}_\xi + \boldsymbol{t}_{\alpha_\xi}\boldsymbol{t}_{\alpha_\xi}^{\mathrm{T}})\boldsymbol{u}_\kappa + (\mathsf{H}_\xi \mathsf{J}_\kappa \boldsymbol{f}_\kappa + \boldsymbol{t}_{\alpha_\xi}(\mathcal{U}_{\mathrm{L}})_\kappa) = \boldsymbol{0}$$

$$\mathsf{H}_\xi \mathsf{J}_\kappa \boldsymbol{e}_{\mathcal{U}_\kappa} - \mathsf{A}_\xi(\boldsymbol{u}_\kappa - (\boldsymbol{u}_h)_\kappa) = \boldsymbol{0},$$

where we have introduced $\mathsf{A}_\xi \equiv \mathsf{Q}_\xi + \boldsymbol{t}_{\alpha_\xi}\boldsymbol{t}_{\alpha_\xi}^{\mathrm{T}}$ (note that from the definition of the discretization of the primal problem we can write $\mathsf{A}_\xi(\boldsymbol{u}_h)_\kappa = \mathsf{H}_\xi \mathsf{J}_\kappa \boldsymbol{f}_\kappa + \boldsymbol{t}_{\alpha_\xi}(\mathcal{U}_{\mathrm{L}})_\kappa$). Adding $(\boldsymbol{\psi}_h)_\kappa^{\mathrm{T}}\boldsymbol{0} = 0 = (\boldsymbol{\psi}_h)_\kappa^{\mathrm{T}}\mathsf{H}_\xi \mathsf{J}_\kappa \boldsymbol{e}_{\mathcal{U}_\kappa} - (\boldsymbol{\psi}_h)_\kappa^{\mathrm{T}}\mathsf{A}_\xi(\boldsymbol{u}_\kappa - (\boldsymbol{u}_h)_\kappa)$ to the discrete integral equation, $\boldsymbol{g}_\kappa^{\mathrm{T}}\mathsf{H}_\xi \mathsf{J}_\kappa(\boldsymbol{u}_\kappa - (\boldsymbol{u}_h)_\kappa)$, gives

$$\boldsymbol{g}_\kappa^{\mathrm{T}}\mathsf{H}_\xi \mathsf{J}_\kappa(\boldsymbol{u}_\kappa - (\boldsymbol{u}_h)_\kappa)$$
$$= \boldsymbol{g}_\kappa^{\mathrm{T}}\mathsf{H}_\xi \mathsf{J}_\kappa(\boldsymbol{u}_\kappa - (\boldsymbol{u}_h)_\kappa) + (\boldsymbol{\psi}_h)_\kappa^{\mathrm{T}}\mathsf{H}_\xi \mathsf{J}_\kappa \boldsymbol{e}_{\mathcal{U}_\kappa} - (\boldsymbol{\psi}_h)_\kappa^{\mathrm{T}}\mathsf{A}_\xi(\boldsymbol{u}_\kappa - (\boldsymbol{u}_h)_\kappa)$$
$$= \boldsymbol{g}_\kappa^{\mathrm{T}}\mathsf{H}_\xi \mathsf{J}_\kappa(\boldsymbol{u}_\kappa - (\boldsymbol{u}_h)_\kappa) - (\boldsymbol{\psi}_h)_\kappa^{\mathrm{T}}\mathsf{A}_\xi \mathsf{J}_\kappa^{-1}\mathsf{H}_\xi^{-1}\mathsf{H}_\xi \mathsf{J}_\kappa(\boldsymbol{u}_\kappa - (\boldsymbol{u}_h)_\kappa) + (\boldsymbol{\psi}_h)_\kappa^{\mathrm{T}}\mathsf{H}_\xi \mathsf{J}_\kappa \boldsymbol{e}_{\mathcal{U}_\kappa}$$
$$= (\boldsymbol{g}_\kappa^{\mathrm{T}} - (\boldsymbol{\psi}_h)_\kappa^{\mathrm{T}}\mathsf{A}_\xi \mathsf{J}_\kappa^{-1}\mathsf{H}_\xi^{-1})\mathsf{H}_\xi \mathsf{J}_\kappa(\boldsymbol{u}_\kappa - (\boldsymbol{u}_h)_\kappa) + (\boldsymbol{\psi}_h)_\kappa^{\mathrm{T}}\mathsf{H}_\xi \mathsf{J}_\kappa \boldsymbol{e}_{\mathcal{U}_\kappa}$$
$$= (\boldsymbol{g}_\kappa - \mathsf{J}_\kappa^{-1}\mathsf{H}_\xi^{-1}\mathsf{A}_\xi^{\mathrm{T}}(\boldsymbol{\psi}_h)_\kappa)^{\mathrm{T}}\mathsf{H}_\xi \mathsf{J}_\kappa(\boldsymbol{u}_\kappa - (\boldsymbol{u}_h)_\kappa) + (\boldsymbol{\psi}_h)_\kappa^{\mathrm{T}}\mathsf{H}_\xi \mathsf{J}_\kappa \boldsymbol{e}_{\mathcal{U}_\kappa}$$
$$= (\boldsymbol{g}_\kappa - \mathsf{J}_\kappa^{-1}\mathsf{H}_\xi^{-1}(-\mathsf{Q}_\xi + \boldsymbol{t}_{\beta_\xi}\boldsymbol{t}_{\beta_\xi}^{\mathrm{T}})(\boldsymbol{\psi}_h)_\kappa)^{\mathrm{T}}\mathsf{H}_\xi \mathsf{J}_\kappa(\boldsymbol{u}_\kappa - (\boldsymbol{u}_h)_\kappa) + (\boldsymbol{\psi}_h)_\kappa^{\mathrm{T}}\mathsf{H}_\xi \mathsf{J}_\kappa \boldsymbol{e}_{\mathcal{U}_\kappa}$$
$$= (\mathsf{J}_\kappa^{-1}\mathsf{D}_\xi(\boldsymbol{\psi}_h)_\kappa + \boldsymbol{g}_\kappa - \mathsf{J}_\kappa^{-1}\mathsf{H}_\xi^{-1}\boldsymbol{t}_{\beta_\xi}\boldsymbol{t}_{\beta_\xi}^{\mathrm{T}}(\boldsymbol{\psi}_h)_\kappa)^{\mathrm{T}}\mathsf{H}_\xi \mathsf{J}_\kappa(\boldsymbol{u}_\kappa - (\boldsymbol{u}_h)_\kappa) + (\boldsymbol{\psi}_h)_\kappa^{\mathrm{T}}\mathsf{H}_\xi \mathsf{J}_\kappa \boldsymbol{e}_{\mathcal{U}_\kappa},$$

or, adding and subtracting $(\psi_{\mathrm{R}})_\kappa(\mathsf{J}_\kappa^{-1}\mathsf{H}_\xi^{-1}\boldsymbol{t}_{\beta_\xi})^{\mathrm{T}}\mathsf{H}_\xi \mathsf{J}_\kappa(\boldsymbol{u}_\kappa - (\boldsymbol{u}_h)_\kappa)$ gives

$$\boldsymbol{g}_\kappa^{\mathrm{T}}\mathsf{H}_\xi \mathsf{J}_\kappa(\boldsymbol{u}_\kappa - (\boldsymbol{u}_h)_\kappa)$$
$$= (\mathsf{J}_\kappa^{-1}\mathsf{D}_\xi(\boldsymbol{\psi}_h)_\kappa + \boldsymbol{g}_\kappa - \mathsf{J}_\kappa^{-1}\mathsf{H}_\xi^{-1}\boldsymbol{t}_{\beta_\xi}(\boldsymbol{t}_{\beta_\xi}^{\mathrm{T}}(\boldsymbol{\psi}_h)_\kappa - (\psi_{\mathrm{R}})_\kappa))^{\mathrm{T}}\mathsf{H}_\xi \mathsf{J}_\kappa(\boldsymbol{u}_\kappa - (\boldsymbol{u}_h)_\kappa)$$
$$\quad - \psi_{\mathrm{R}}(\mathsf{J}_\kappa^{-1}\mathsf{H}_\xi^{-1}\boldsymbol{t}_{\beta_\xi})^{\mathrm{T}}\mathsf{H}_\xi \mathsf{J}_\kappa(\boldsymbol{u}_\kappa - (\boldsymbol{u}_h)_\kappa) + (\boldsymbol{\psi}_h)_\kappa^{\mathrm{T}}\mathsf{H}_\xi \mathsf{J}_\kappa \boldsymbol{e}_{\mathcal{U}_\kappa}$$
$$= -(\psi_{\mathrm{R}})_\kappa(\mathsf{J}_\kappa^{-1}\mathsf{H}_\xi^{-1}\boldsymbol{t}_{\beta_\xi})^{\mathrm{T}}\mathsf{H}_\xi \mathsf{J}_\kappa(\boldsymbol{u}_\kappa - (\boldsymbol{u}_h)_\kappa) + (\boldsymbol{\psi}_h)_\kappa^{\mathrm{T}}\mathsf{H}_\xi \mathsf{J}_\kappa \boldsymbol{e}_{\mathcal{U}_\kappa}$$

where the first term in the penultimate step is zero due to the definition of the discretization of the dual problem. Continuing by adding and subtracting $\boldsymbol{\psi}_\kappa^{\mathrm{T}}\mathsf{H}_\xi \mathsf{J}_\kappa \boldsymbol{e}_{\mathcal{U}_\kappa}$, we have

$$\boldsymbol{g}_\kappa^{\mathrm{T}}\mathsf{H}_\xi \mathsf{J}_\kappa(\boldsymbol{u}_\kappa - (\boldsymbol{u}_h)_\kappa)$$
$$= -(\psi_{\mathrm{R}})_\kappa(\mathsf{J}_\kappa^{-1}\mathsf{H}_\xi^{-1}\boldsymbol{t}_{\beta_\xi})^{\mathrm{T}}\mathsf{H}_\xi \mathsf{J}_\kappa(\boldsymbol{u}_\kappa - (\boldsymbol{u}_h)_\kappa) + (\boldsymbol{\psi}_h)_\kappa^{\mathrm{T}}\mathsf{H}_\xi \mathsf{J}_\kappa \boldsymbol{e}_{\mathcal{U}_\kappa}$$
$$\quad + \boldsymbol{\psi}_\kappa^{\mathrm{T}}\mathsf{H}_\xi \mathsf{J}_\kappa \boldsymbol{e}_{\mathcal{U}_\kappa} - \boldsymbol{\psi}_\kappa^{\mathrm{T}}\mathsf{H}_\xi \mathsf{J}_\kappa \boldsymbol{e}_{\mathcal{U}_\kappa}$$
$$= ((\boldsymbol{\psi}_h)_\kappa - \boldsymbol{\psi}_\kappa)^{\mathrm{T}}\mathsf{H}_\xi \mathsf{J}_\kappa \boldsymbol{e}_{\mathcal{U}_\kappa} + \boldsymbol{\psi}^{\mathrm{T}}\mathsf{H}_\xi \mathsf{J}_\kappa \boldsymbol{e}_{\mathcal{U}_\kappa} - (\psi_{\mathrm{R}})_\kappa \boldsymbol{t}_{\beta_\xi}^{\mathrm{T}}(\boldsymbol{u}_\kappa - (\boldsymbol{u}_h)_\kappa).$$

However, note that $\mathsf{A}_\xi^{\mathrm{T}}(\boldsymbol{\psi}_\kappa - (\boldsymbol{\psi}_h)_\kappa) = \mathsf{H}_\xi \mathsf{J}_\kappa \boldsymbol{e}_{\psi_\kappa}$, which means

$$\boldsymbol{g}_\kappa^{\mathrm{T}} \mathsf{H}_\xi \mathsf{J}_\kappa (\boldsymbol{u}_\kappa - (\boldsymbol{u}_h)_\kappa)$$
$$= -(\mathsf{A}_\xi^{-\mathrm{T}} \mathsf{H}_\xi \mathsf{J}_\kappa \boldsymbol{e}_{\psi_\kappa})^{\mathrm{T}} \mathsf{H}_\xi \mathsf{J}_\kappa \boldsymbol{e}_{\mathcal{U}_\kappa} + \boldsymbol{\psi}_\kappa^{\mathrm{T}} \mathsf{H}_\xi \mathsf{J}_\kappa \boldsymbol{e}_{\mathcal{U}_\kappa} - (\psi_{\mathrm{R}})_\kappa \boldsymbol{t}_{\beta_\xi}^{\mathrm{T}} (\boldsymbol{u}_\kappa - (\boldsymbol{u}_h)_\kappa).$$

Furthermore, making the assumption that $\left\| \mathsf{A}_\xi^{-\mathrm{T}} \mathsf{H}_\xi \right\|_\infty \leq C$, where C is a constant, gives

$$\boldsymbol{g}_\kappa^{\mathrm{T}} \mathsf{H}_\xi \mathsf{J}_\kappa (\boldsymbol{u}_\kappa - (\boldsymbol{u}_h)_\kappa) = \boldsymbol{\psi}_\kappa^{\mathrm{T}} \mathsf{H}_\xi \mathsf{J}_\kappa \boldsymbol{e}_{\mathcal{U}_\kappa} - (\psi_{\mathrm{R}})_\kappa \boldsymbol{t}_{\beta_\xi}^{\mathrm{T}} (\boldsymbol{u}_\kappa - (\boldsymbol{u}_h)_\kappa) + \mathcal{O}(h^{\tau+1}).$$

Note that the justification for assuming $\left\| \mathsf{A}_\xi^{-\mathrm{T}} \mathsf{H}_\xi \right\|_\infty \leq C$ is thoroughly discussed in [20]. Continuing with our analysis, we can substitute the expression for $\boldsymbol{e}_{\mathcal{U}_\kappa}$ into the above and write,

$$\boldsymbol{g}_\kappa^{\mathrm{T}} \mathsf{H}_\xi \mathsf{J}_\kappa (\boldsymbol{u}_\kappa - (\boldsymbol{u}_h)_\kappa) = \boldsymbol{\psi}_\kappa^{\mathrm{T}} \mathsf{H}_\xi \mathsf{J}_\kappa \boldsymbol{e}_{\mathcal{U}_\kappa} - (\psi_{\mathrm{R}})_\kappa \boldsymbol{t}_{\beta_\xi}^{\mathrm{T}} (\boldsymbol{u}_\kappa - (\boldsymbol{u}_h)_\kappa) + \mathcal{O}(h^{\tau+1})$$
$$= \boldsymbol{\psi}_\kappa^{\mathrm{T}} \mathsf{H}_\xi \mathsf{J}_\kappa (\mathsf{J}_\kappa^{-1} \mathsf{D}_\xi \boldsymbol{u}_\kappa + \mathsf{J}_\kappa^{-1} \mathsf{H}_\xi^{-1} \boldsymbol{t}_{\alpha_\xi} (\boldsymbol{t}_{\alpha_\xi}^{\mathrm{T}} \boldsymbol{u}_\kappa - (\mathcal{U}_{\mathrm{L}})_\kappa))$$
$$\quad - (\psi_{\mathrm{R}})_\kappa \boldsymbol{t}_{\beta_\xi}^{\mathrm{T}} (\boldsymbol{u}_\kappa - (\boldsymbol{u}_h)_\kappa) - \boldsymbol{\psi}_\kappa^{\mathrm{T}} \mathsf{H}_\xi \mathsf{J}_\kappa \boldsymbol{f}_\kappa + \mathcal{O}(h^{\tau+1})$$
$$= \boldsymbol{\psi}_\kappa^{\mathrm{T}} \mathsf{H}_\xi \mathsf{J}_\kappa (\mathsf{J}_\kappa^{-1} \mathsf{D}_\xi \boldsymbol{u}_\kappa + \mathsf{J}_\kappa^{-1} \mathsf{H}_\xi^{-1} \boldsymbol{t}_{\alpha_\xi} (\boldsymbol{t}_{\alpha_\xi}^{\mathrm{T}} \boldsymbol{u}_\kappa - (\mathcal{U}_{\mathrm{L}})_\kappa))$$
$$\quad - (\psi_{\mathrm{R}})_\kappa \boldsymbol{t}_{\beta_\xi}^{\mathrm{T}} (\boldsymbol{u}_\kappa - (\boldsymbol{u}_h)_\kappa) - \int_{(\hat{\Omega}_\xi)_\kappa} \psi_\kappa \frac{d\mathcal{U}_\kappa}{d\xi} \, d\hat{\Omega}_\xi + \mathcal{O}(h^{\tau+1}).$$

Furthermore, using Lemma 2, we can substitute $\boldsymbol{t}_{\beta_\xi}^{\mathrm{T}} (\boldsymbol{u}_h)_\kappa = (\mathcal{U}_{\mathrm{R}})_\kappa + \mathcal{O}(h^{\tau+1})$ into the preceding expression and write, using Lemma 3,

$$\boldsymbol{g}_\kappa^{\mathrm{T}} \mathsf{H}_\xi \mathsf{J}_\kappa (\boldsymbol{u}_\kappa - (\boldsymbol{u}_h)_\kappa) = \boldsymbol{\psi}_\kappa^{\mathrm{T}} \mathsf{H}_\xi (\mathsf{D}_\xi \boldsymbol{u}_\kappa + \mathsf{H}_\xi^{-1} \boldsymbol{t}_{\alpha_\xi} (\boldsymbol{t}_{\alpha_\xi}^{\mathrm{T}} \boldsymbol{u}_\kappa - (\mathcal{U}_{\mathrm{L}})_\kappa)) - (\psi_{\mathrm{R}})_\kappa \boldsymbol{t}_{\beta_\xi}^{\mathrm{T}} \boldsymbol{u}_\kappa$$
$$\quad + (\psi_{\mathrm{R}})_\kappa (\mathcal{U}_{\mathrm{R}})_\kappa - \int_{(\hat{\Omega}_\xi)_\kappa} \psi_\kappa \frac{d\mathcal{U}_\kappa}{d\xi} \, d\hat{\Omega}_\xi + \mathcal{O}(h^{\tau+1}).$$
$$= \mathcal{O}(h^{\min(2p+1, \tau+1)}) + \mathcal{O}(h^{\tau+1})$$
$$= \mathcal{O}(h^{\min(2p+1, \tau+1)})$$

We have shown that, for the κth element,

$$\int_{(\hat{\Omega}_\xi)_\kappa} \mathcal{G}_\kappa \mathcal{U}_\kappa \mathcal{J}_\kappa \, d\hat{\Omega}_\xi - \boldsymbol{g}_\kappa^{\mathrm{T}} \mathsf{H}_\xi \mathsf{J}_\kappa (\boldsymbol{u}_h)_\kappa = \mathcal{O}(h^{\min(2p+1, \tau+1)}). \tag{17}$$

Substituting (15) and (17) into (14) gives

$$\mathcal{I}(\mathcal{U}) - \mathcal{I}_h(\boldsymbol{u}_h) = \sum_{\kappa=1}^{K} \left(\mathcal{O}(h^{\min(2p+1, \tau+1)}) \right) + \mathcal{O}(h^{\tau+1})$$
$$= \mathcal{O}(h^{\min(2p+1, \tau+1)}).$$

Therefore, we have shown,

$$\mathcal{I}(\mathcal{U}) - \mathcal{I}_h(\mathcal{U}) = \mathcal{O}(h^{\min(2p+1, \tau+1)}),$$

which concludes the proof. $\qquad\square$

To summarize, thus far we have seen that, under Assumption 2, we can obtain superconvergent linear functionals for generalized SBP operators in curvilinear coordinates. In practice, if Assumption 2 is violated, this means that interpolation/extrapolation operators of degree $r \geq 2p$ are required to preserve quadrature accuracy and functional superconvergence in curvilinear coordinates when: (1) the Jacobian of the transformation is approximated using the same SBP operator that is associated with the norm, and (2) a higher degree representation of the geometry is used compared to the degree of the corresponding SBP operator.

4.3 Interface simultaneous-approximation-terms

Until now, our analysis has been focused on a specific element, i.e., the κth element (or element K). Here, we show that the interface SATs between elements do not affect functional superconvergence. We follow a procedure similar to [20]. Consider partitioning Ω into two elements. The discretizations for the first and second elements are given as

$$\mathsf{J}_1^{-1}\mathsf{D}_\xi(\boldsymbol{u}_h)_1 = \boldsymbol{f}_1 - \mathsf{J}_1^{-1}\mathsf{H}_\xi^{-1}\boldsymbol{t}_{\alpha_\xi}(\boldsymbol{t}_{\alpha_\xi}^{\mathrm{T}}(\boldsymbol{u}_h)_1 - \mathcal{U}_{\mathrm{L}}) + \sigma_1\boldsymbol{t}_{\beta_\xi}(\boldsymbol{t}_{\beta_\xi}^{\mathrm{T}}(\boldsymbol{u}_h)_1 - \boldsymbol{t}_{\alpha_\xi}^{\mathrm{T}}(\boldsymbol{u}_h)_2)$$

and

$$\mathsf{J}_2^{-1}\mathsf{D}_\xi(\boldsymbol{u}_h)_2 = \boldsymbol{f}_2 + \sigma_2\boldsymbol{t}_{\alpha_\xi}(\boldsymbol{t}_{\alpha_\xi}^{\mathrm{T}}(\boldsymbol{u}_h)_2 - \boldsymbol{t}_{\beta_\xi}^{\mathrm{T}}(\boldsymbol{u}_h)_1),$$

respectively, where σ_1 and σ_2 are scalars. To determine permissible values for σ_1 and σ_2, we expand (13) for our two-element example and add the discrete residual for each element. This gives

$$\begin{aligned}\mathcal{I}_h(\boldsymbol{u}_h) = {}&\boldsymbol{g}_1^{\mathrm{T}}\mathsf{H}_\xi\mathsf{J}_1(\boldsymbol{u}_h)_1 + \boldsymbol{g}_2^{\mathrm{T}}\mathsf{H}_\xi\mathsf{J}_2(\boldsymbol{u}_h)_2 + \psi_{\mathrm{R}}\boldsymbol{t}_{\beta_\xi}^{\mathrm{T}}(\boldsymbol{u}_h)_2 \\ &+ \mathsf{R}_h((\boldsymbol{u}_h)_1,(\boldsymbol{\psi}_h)_1) + \mathsf{R}_h((\boldsymbol{u}_h)_2,(\boldsymbol{\psi}_h)_2),\end{aligned}$$

or, after some algebra,

$$\begin{aligned}\mathcal{I}_h(\boldsymbol{u}_h) = {}&(\boldsymbol{\psi}_h)_1^{\mathrm{T}}\mathsf{H}_\xi\mathsf{J}_1\boldsymbol{f}_1 + (\boldsymbol{\psi}_h)_2^{\mathrm{T}}\mathsf{H}_\xi\mathsf{J}_2\boldsymbol{f}_2 + (\boldsymbol{\psi}_h)_1^{\mathrm{T}}\boldsymbol{t}_{\alpha_\xi}\mathcal{U}_{\mathrm{L}} \\ &+ \mathsf{R}_h^*((\boldsymbol{\psi}_h)_1,(\boldsymbol{u}_h)_1) + \mathsf{R}_h^*((\boldsymbol{\psi}_h)_2,(\boldsymbol{u}_h)_2),\end{aligned}$$

where

$$\begin{aligned}\mathsf{R}_h^*((\boldsymbol{\psi}_h)_1,(\boldsymbol{u}_h)_1) = {}&(\boldsymbol{u}_h)_1^{\mathrm{T}}\mathsf{H}_\xi\mathsf{J}_1\Big(\boldsymbol{g}_1 + \mathsf{J}_1^{-1}\mathsf{D}_\xi(\boldsymbol{\psi}_h)_1 \\ &- \mathsf{J}_1^{-1}\mathsf{H}_\xi^{-1}\boldsymbol{t}_{\beta_\xi}((1-\sigma_1)\boldsymbol{t}_{\beta_\xi}^{\mathrm{T}}(\boldsymbol{\psi}_h)_1 - (-\sigma_2)\boldsymbol{t}_{\alpha_\xi}^{\mathrm{T}}(\boldsymbol{\psi}_h)_2)\Big)\end{aligned}$$

and

$$\begin{aligned}\mathsf{R}_h^*((\boldsymbol{\psi}_h)_2,(\boldsymbol{u}_h)_2) = {}&(\boldsymbol{u}_h)_2^{\mathrm{T}}\mathsf{H}_\xi\mathsf{J}_2\Big(\boldsymbol{g}_2 + \mathsf{J}_2^{-1}\mathsf{D}_\xi(\boldsymbol{\psi}_h)_2 \\ &- \mathsf{J}_2^{-1}\mathsf{H}_\xi^{-1}\boldsymbol{t}_{\alpha_\xi}(-(\sigma_2+1)\boldsymbol{t}_{\alpha_\xi}^{\mathrm{T}}(\boldsymbol{\psi}_h)_2 - (-\sigma_1)\boldsymbol{t}_{\beta_\xi}^{\mathrm{T}}(\boldsymbol{\psi}_h)_1) \\ &- \mathsf{J}_2^{-1}\mathsf{H}_\xi^{-1}\boldsymbol{t}_{\beta_\xi}(\boldsymbol{t}_{\beta_\xi}^{\mathrm{T}}(\boldsymbol{\psi}_h)_2 - \psi_{\mathrm{R}})\Big).\end{aligned}$$

Examining the dual residuals $\mathsf{R}_h^*((\boldsymbol{\psi}_h)_1, (\boldsymbol{u}_h)_1)$ and $\mathsf{R}_h^*((\boldsymbol{\psi}_h)_2, (\boldsymbol{u}_h)_2)$, we see that, for dual consistency, we must have $\sigma_1 = \sigma_2 + 1$, which can also lead to stability and conservation. This is the same conclusion reached in [20]; however here we have performed this analysis for generalized SBP operators in curvilinear coordinates. This analysis confirms that our choice of interface penalties does not affect functional superconvergence. For $K > 2$, this analysis generalizes through the condition $\sigma_\kappa = \sigma_{\kappa+1} + 1$. It is common to select

$$\sigma_\kappa = \frac{1}{2}(1 - \sigma)$$

$$\sigma_{\kappa+1} = -\frac{1}{2}(1 + \sigma),$$

where $\sigma = 0$ gives symmetric interface SATs and $\sigma = 1$ returns upwind interface SATs. Throughout this work, we exclusively use upwind interface SATs, as symmetric interface SATs can sometimes lead to suboptimal convergence of the numerical solution [14], although both alternatives can enable dual consistent schemes.

4.4 Discretization in multiple dimensions

Here we sketch the extension to a two-dimensional discretization. Consider the two-dimensional boundary-value problem on the square $\Omega \equiv [\alpha_x, \beta_x] \times [\alpha_y, \beta_y]$

$$\begin{aligned}
\nabla \cdot (\boldsymbol{a}\mathcal{U}) &= \mathcal{F} \quad &\forall (x, y) \in \Omega \\
\mathcal{U} &= \mathcal{U}^- \quad &\forall (x, y) \in \Gamma^-,
\end{aligned} \tag{18}$$

where $\nabla = [\partial/\partial x, \partial/\partial y]^{\mathrm{T}}$, $\boldsymbol{a} = [a_x, a_y]^{\mathrm{T}}$ (with $a_x \in \mathbb{R}_{>0}$ and $a_y \in \mathbb{R}_{>0}$), $\mathcal{F} \in L^2(\Omega)$, and $\Gamma^- \equiv \{(x, y) \in \Gamma \mid \boldsymbol{a} \cdot \boldsymbol{n} \le 0\}$ denotes the inflow boundary. We consider the linear functional

$$\mathcal{I}(\mathcal{U}) = \oint_{\Gamma^+} \psi^+ \boldsymbol{n} \cdot (\boldsymbol{a}\mathcal{U}) \, d\Gamma,$$

which is defined over the outflow boundary of Ω, $\Gamma^+ \equiv \Gamma \setminus \Gamma^-$, where $\psi^+ \in \mathbb{R}$ and $\boldsymbol{n} = [n_x, n_y]^{\mathrm{T}}$. Note that in this case, $\Gamma^- = \Gamma^{\alpha_\xi} \cup \Gamma^{\alpha_\eta}$ and $\Gamma^+ = \Gamma^{\beta_\xi} \cup \Gamma^{\beta_\eta}$.

Transforming (18) to the reference element gives, on the κth element,

$$\tilde{\nabla} \cdot (\tilde{\boldsymbol{a}}\mathcal{U}) = \mathcal{J}_\kappa \mathcal{F}_\kappa, \tag{19}$$

where $\tilde{\nabla} = [\partial/\partial \xi, \partial/\partial \eta]^{\mathrm{T}}$ and $\tilde{\boldsymbol{a}} = [\lambda_\xi, \lambda_\eta]^{\mathrm{T}}$. Here,

$$\lambda_\xi = \mathcal{J}_\kappa \left(a_x \frac{\partial \xi}{\partial x_\kappa} + a_y \frac{\partial \xi}{\partial y_\kappa} \right) = a_x \frac{\partial y_\kappa}{\partial \eta} - a_y \frac{\partial x_\kappa}{\partial \eta}$$

$$\lambda_\eta = \mathcal{J}_\kappa \left(a_x \frac{\partial \eta}{\partial x_\kappa} + a_y \frac{\partial \eta}{\partial y_\kappa} \right) = -a_x \frac{\partial y_\kappa}{\partial \xi} + a_y \frac{\partial x_\kappa}{\partial \xi},$$

where

$$\mathcal{J}_\kappa \equiv \frac{\partial x_\kappa}{\partial \xi}\frac{\partial y_\kappa}{\partial \eta} - \frac{\partial y_\kappa}{\partial \xi}\frac{\partial x_\kappa}{\partial \eta}.$$

We can also write our functional in terms of the reference element as

$$\mathcal{I}(\mathcal{U}) = \sum_{\gamma \subset \varGamma^+} \left(\oint_{\hat{\gamma}} \psi^+ \tilde{\boldsymbol{n}} \cdot (\tilde{\boldsymbol{a}}\mathcal{U}_\kappa)\, d\hat{\varGamma} \right), \tag{20}$$

where $\tilde{\boldsymbol{n}} = [n_\xi, n_\eta]^{\mathrm{T}}$, $\gamma \subset \varGamma_\kappa$ denotes a facet that coincides with $\varGamma^+$, and $\hat{\gamma} \subset \hat{\varGamma}_\kappa$ is the corresponding facet in reference space.

On the κth element, the discretization of (19), using upwind SATs, is given by

$$\begin{aligned}
\tilde{\mathsf{D}}_\xi(\Lambda_\xi)_\kappa(\boldsymbol{u}_h)_\kappa &+ \tilde{\mathsf{D}}_\eta(\Lambda_\eta)_\kappa(\boldsymbol{u}_h)_\kappa = \mathsf{J}_\kappa \boldsymbol{f}_\kappa \\
&- \tilde{\mathsf{H}}^{-1}\tilde{\mathsf{R}}_{\alpha_\xi}^{\mathrm{T}}\tilde{\mathsf{H}}_\xi^\perp(\tilde{\mathsf{R}}_{\alpha_\xi}(\Lambda_\xi)_\kappa(\boldsymbol{u}_h)_\kappa - (\lambda_\xi \mathcal{U}_{\mathrm{West}})_\kappa) \\
&- \tilde{\mathsf{H}}^{-1}\tilde{\mathsf{R}}_{\alpha_\eta}^{\mathrm{T}}\tilde{\mathsf{H}}_\eta^\perp(\tilde{\mathsf{R}}_{\alpha_\eta}(\Lambda_\eta)_\kappa(\boldsymbol{u}_h)_\kappa - (\lambda_\eta \mathcal{U}_{\mathrm{South}})_\kappa),
\end{aligned} \tag{21}$$

where

$$\begin{aligned}
(\Lambda_\xi)_\kappa &\equiv \mathrm{diag}(a_x \tilde{\mathsf{D}}_\eta \boldsymbol{y}_\kappa - a_y \tilde{\mathsf{D}}_\eta \boldsymbol{x}_\kappa) \\
(\Lambda_\eta)_\kappa &\equiv \mathrm{diag}(-a_x \tilde{\mathsf{D}}_\xi \boldsymbol{y}_\kappa + a_y \tilde{\mathsf{D}}_\xi \boldsymbol{x}_\kappa).
\end{aligned}$$

Furthermore, the Jacobian of the transformation is constructed as

$$\mathsf{J}_\kappa = \mathrm{diag}(\mathrm{diag}(\tilde{\mathsf{D}}_\xi \boldsymbol{x}_\kappa)\tilde{\mathsf{D}}_\eta \boldsymbol{y}_\kappa - \mathrm{diag}(\tilde{\mathsf{D}}_\eta \boldsymbol{x}_\kappa)\tilde{\mathsf{D}}_\xi \boldsymbol{y}_\kappa),$$

where this specific form has been used to satisfy the metric invariants [35]. When the κth element borders either the South and/or West boundaries of $\varOmega$, then

$$(\lambda_\eta \mathcal{U}_{\mathrm{South}})_\kappa = \tilde{\mathsf{R}}_{\alpha_\eta}(\Lambda_\eta)_\kappa(\mathsf{I}_\xi \otimes \mathbf{1}_\eta)\mathcal{U}_{\mathrm{South}}(\boldsymbol{\xi}^{\alpha_\eta})$$

and/or

$$(\lambda_\xi \mathcal{U}_{\mathrm{West}})_\kappa = \tilde{\mathsf{R}}_{\alpha_\xi}(\Lambda_\xi)_\kappa(\mathbf{1}_\xi \otimes \mathsf{I}_\eta)\mathcal{U}_{\mathrm{West}}(\boldsymbol{\eta}^{\alpha_\xi}),$$

respectively. Alternatively, when the κth element does *not* border either the South and/or West boundaries of $\varOmega$, then

$$(\lambda_\eta \mathcal{U}_{\mathrm{South}})_\kappa = \tilde{\mathsf{R}}_{\beta_\eta}(\Lambda_\eta)_{\kappa,\mathrm{South}}(\boldsymbol{u}_h)_{\kappa,\mathrm{South}}$$

and/or

$$(\lambda_\xi \mathcal{U}_{\mathrm{West}})_\kappa = \tilde{\mathsf{R}}_{\beta_\xi}(\Lambda_\xi)_{\kappa,\mathrm{West}}(\boldsymbol{u}_h)_{\kappa,\mathrm{West}},$$

respectively, where the subscripts South and West denote quantities computed with information from the South and West elements relative to the κth element, respectively.

We can approximate our continuous functional as

$$\mathcal{I}_h(\boldsymbol{u}_h) = \sum_{\gamma \subset \varGamma^+} \left(\psi^+ \mathbf{1}^{\mathrm{T}} \tilde{\mathsf{E}}_{\hat{\gamma}}(\boldsymbol{u}_h)_\kappa \right), \tag{22}$$

where, in this case, either $\tilde{\mathsf{E}}_{\hat\gamma} = \tilde{\mathsf{E}}_{\beta_\xi}(\Lambda_\xi)_\kappa$ or $\tilde{\mathsf{E}}_{\hat\gamma} = \tilde{\mathsf{E}}_{\beta_\eta}(\Lambda_\eta)_\kappa$, depending on the specific facet we are on. As in the one-dimensional case, we are interested in how well $\mathcal{I}_h(\boldsymbol{u}_h)$ approximates $\mathcal{I}(\mathcal{U})$. To this end, we introduce the following lemmas.

Lemma 4 *For each element $\kappa = 1, 2, \ldots, K$, using Assumption 2, the term*

$$\mathbf{1}^{\mathrm{T}}\tilde{\mathsf{E}}_{\beta_\xi}(\Lambda_\xi)_\kappa(\boldsymbol{u}_h)_\kappa + \mathbf{1}^{\mathrm{T}}\tilde{\mathsf{E}}_{\beta_\eta}(\Lambda_\eta)_\kappa(\boldsymbol{u}_h)_\kappa$$

is a degree τ and order $\tau + 1$ approximation of

$$\int_{\hat{\Gamma}_\kappa^+} \tilde{\boldsymbol{n}} \cdot (\tilde{\boldsymbol{a}}\mathcal{U}_\kappa)\, d\hat{\Gamma} \equiv \int_{\hat{\Gamma}_\kappa^{\beta_\xi}} \tilde{\boldsymbol{n}} \cdot (\tilde{\boldsymbol{a}}\mathcal{U}_\kappa)\, d\hat{\Gamma} + \int_{\hat{\Gamma}_\kappa^{\beta_\eta}} \tilde{\boldsymbol{n}} \cdot (\tilde{\boldsymbol{a}}\mathcal{U}_\kappa)\, d\hat{\Gamma},$$

where $\mathcal{U}_\kappa \in C^{\tau+1}(\hat{\Omega}_\kappa)$.

Proof Let

$$\int_{\hat{\Gamma}_\kappa^-} \tilde{\boldsymbol{n}} \cdot (\tilde{\boldsymbol{a}}\mathcal{U}_\kappa)\, d\hat{\Gamma} \equiv \int_{\hat{\Gamma}_\kappa^{\alpha_\xi}} \tilde{\boldsymbol{n}} \cdot (\tilde{\boldsymbol{a}}\mathcal{U}_\kappa)\, d\hat{\Gamma} + \int_{\hat{\Gamma}_\kappa^{\alpha_\eta}} \tilde{\boldsymbol{n}} \cdot (\tilde{\boldsymbol{a}}\mathcal{U}_\kappa)\, d\hat{\Gamma}.$$

Then, we have

$$\int_{\hat{\Gamma}_\kappa^+} \tilde{\boldsymbol{n}} \cdot (\tilde{\boldsymbol{a}}\mathcal{U}_\kappa)\, d\hat{\Gamma} - \mathbf{1}^{\mathrm{T}}\tilde{\mathsf{E}}_{\beta_\xi}(\Lambda_\xi)_\kappa(\boldsymbol{u}_h)_\kappa - \mathbf{1}^{\mathrm{T}}\tilde{\mathsf{E}}_{\beta_\eta}(\Lambda_\eta)_\kappa(\boldsymbol{u}_h)_\kappa$$

$$= \int_{\hat{\Gamma}_\kappa} \tilde{\boldsymbol{n}} \cdot (\tilde{\boldsymbol{a}}\mathcal{U}_\kappa)\, d\hat{\Gamma} - \int_{\hat{\Gamma}_\kappa^-} \tilde{\boldsymbol{n}} \cdot (\tilde{\boldsymbol{a}}\mathcal{U}_\kappa)\, d\hat{\Gamma} - \mathbf{1}^{\mathrm{T}}(\tilde{\mathsf{E}}_{\beta_\xi}(\Lambda_\xi)_\kappa + \tilde{\mathsf{E}}_{\beta_\eta}(\Lambda_\eta)_\kappa)(\boldsymbol{u}_h)_\kappa$$

$$= \int_{\hat{\Omega}_\kappa} \tilde{\nabla} \cdot (\tilde{\boldsymbol{a}}\mathcal{U}_\kappa)\, d\hat{\Omega} - \int_{\hat{\Gamma}_\kappa^-} \tilde{\boldsymbol{n}} \cdot (\tilde{\boldsymbol{a}}\mathcal{U}_\kappa)\, d\hat{\Gamma} - \mathbf{1}^{\mathrm{T}}(\tilde{\mathsf{E}}_{\beta_\xi}(\Lambda_\xi)_\kappa + \tilde{\mathsf{E}}_{\beta_\eta}(\Lambda_\eta)_\kappa)(\boldsymbol{u}_h)_\kappa$$

$$= \int_{\hat{\Omega}_\kappa} \mathcal{J}_\kappa \mathcal{F}_\kappa\, d\hat{\Omega} - \int_{\hat{\Gamma}_\kappa^-} \tilde{\boldsymbol{n}} \cdot (\tilde{\boldsymbol{a}}\mathcal{U}_\kappa)\, d\hat{\Gamma} - \mathbf{1}^{\mathrm{T}}(\tilde{\mathsf{E}}_{\beta_\xi}(\Lambda_\xi)_\kappa + \tilde{\mathsf{E}}_{\beta_\eta}(\Lambda_\eta)_\kappa)(\boldsymbol{u}_h)_\kappa$$

$$= \mathbf{1}^{\mathrm{T}}\tilde{\mathsf{H}}\mathsf{J}_\kappa \boldsymbol{f}_\kappa + \mathbf{1}^{\mathrm{T}}(\tilde{\mathsf{R}}_{\alpha_\xi}^{\mathrm{T}}\tilde{\mathsf{H}}_\xi^\perp(\lambda_\xi\mathcal{U}_{\mathrm{West}})_\kappa + \tilde{\mathsf{R}}_{\alpha_\eta}^{\mathrm{T}}\tilde{\mathsf{H}}_\eta^\perp(\lambda_\eta\mathcal{U}_{\mathrm{South}})_\kappa)$$
$$\quad - \mathbf{1}^{\mathrm{T}}(\tilde{\mathsf{E}}_{\beta_\xi}(\Lambda_\xi)_\kappa + \tilde{\mathsf{E}}_{\beta_\eta}(\Lambda_\eta)_\kappa)(\boldsymbol{u}_h)_\kappa + \mathcal{O}(h^{\tau+1}),$$

using Assumption 2 and the accuracy of the various norm matrices. Also, from the definition of the discretization of the PDE we have

$$\tilde{\mathsf{H}}\mathsf{J}_\kappa \boldsymbol{f}_\kappa + \tilde{\mathsf{R}}_{\alpha_\xi}^{\mathrm{T}}\tilde{\mathsf{H}}_\xi^\perp(\lambda_\xi\mathcal{U}_{\mathrm{West}})_\kappa + \tilde{\mathsf{H}}^{-1}\tilde{\mathsf{R}}_{\alpha_\eta}^{\mathrm{T}}\tilde{\mathsf{H}}_\eta^\perp(\lambda_\eta\mathcal{U}_{\mathrm{South}})_\kappa$$
$$= (\tilde{\mathsf{H}}\tilde{\mathsf{D}}_\xi(\Lambda_\xi)_\kappa + \tilde{\mathsf{H}}\tilde{\mathsf{D}}_\eta(\Lambda_\eta)_\kappa + \tilde{\mathsf{R}}_{\alpha_\xi}^{\mathrm{T}}\tilde{\mathsf{H}}_\xi^\perp\tilde{\mathsf{R}}_{\alpha_\xi}(\Lambda_\xi)_\kappa + \tilde{\mathsf{R}}_{\alpha_\eta}^{\mathrm{T}}\tilde{\mathsf{H}}_\eta^\perp\tilde{\mathsf{R}}_{\alpha_\eta}(\Lambda_\eta)_\kappa)(\boldsymbol{u}_h)_\kappa$$

and using the SBP property gives

$$\tilde{\mathsf{H}}\mathsf{J}_\kappa \boldsymbol{f}_\kappa + \tilde{\mathsf{R}}_{\alpha_\xi}^{\mathrm{T}}\tilde{\mathsf{H}}_\xi^\perp(\lambda_\xi\mathcal{U}_{\mathrm{West}})_\kappa + \tilde{\mathsf{H}}^{-1}\tilde{\mathsf{R}}_{\alpha_\eta}^{\mathrm{T}}\tilde{\mathsf{H}}_\eta^\perp(\lambda_\eta\mathcal{U}_{\mathrm{South}})_\kappa$$
$$= (-\tilde{\mathsf{Q}}_\xi^{\mathrm{T}}(\Lambda_\xi)_\kappa - \tilde{\mathsf{Q}}_\eta^{\mathrm{T}}(\Lambda_\eta)_\kappa + \tilde{\mathsf{R}}_{\beta_\xi}^{\mathrm{T}}\tilde{\mathsf{H}}_\xi^\perp\tilde{\mathsf{R}}_{\beta_\xi}(\Lambda_\xi)_\kappa + \tilde{\mathsf{R}}_{\beta_\eta}^{\mathrm{T}}\tilde{\mathsf{H}}_\eta^\perp\tilde{\mathsf{R}}_{\beta_\eta}(\Lambda_\eta)_\kappa)(\boldsymbol{u}_h)_\kappa.$$

Therefore,

$$\int_{\hat{\Gamma}_\kappa^+} \tilde{\boldsymbol{n}} \cdot (\tilde{\boldsymbol{a}} \mathcal{U}_\kappa)\, d\hat{\Gamma} - \mathbf{1}^{\mathrm{T}} \tilde{\mathsf{E}}_{\beta_\xi} (\Lambda_\xi)_\kappa (\boldsymbol{u}_h)_\kappa - \mathbf{1}^{\mathrm{T}} \tilde{\mathsf{E}}_{\beta_\eta} (\Lambda_\eta)_\kappa (\boldsymbol{u}_h)_\kappa$$

$$= \mathbf{1}^{\mathrm{T}} (\tilde{\mathsf{H}} \mathsf{J}_\kappa \boldsymbol{f}_\kappa + \tilde{\mathsf{R}}_{\alpha_\xi}^{\mathrm{T}} \tilde{\mathsf{H}}_\xi^\perp (\lambda_\xi \mathcal{U}_{\text{West}})_\kappa + \tilde{\mathsf{R}}_{\alpha_\eta}^{\mathrm{T}} \tilde{\mathsf{H}}_\eta^\perp (\lambda_\eta \mathcal{U}_{\text{South}})_\kappa)$$

$$\quad - \mathbf{1}^{\mathrm{T}} (\tilde{\mathsf{E}}_{\beta_\xi} (\Lambda_\xi)_\kappa + \tilde{\mathsf{E}}_{\beta_\eta} (\Lambda_\eta)_\kappa)(\boldsymbol{u}_h)_\kappa + \mathcal{O}(h^{\tau+1})$$

$$= \mathbf{1}^{\mathrm{T}} (-\tilde{\mathsf{Q}}_\xi^{\mathrm{T}} (\Lambda_\xi)_\kappa - \tilde{\mathsf{Q}}_\eta^{\mathrm{T}} (\Lambda_\eta)_\kappa + \tilde{\mathsf{R}}_{\beta_\xi}^{\mathrm{T}} \tilde{\mathsf{H}}_\xi^\perp \tilde{\mathsf{R}}_{\beta_\xi} (\Lambda_\xi)_\kappa + \tilde{\mathsf{R}}_{\beta_\eta}^{\mathrm{T}} \tilde{\mathsf{H}}_\eta^\perp \tilde{\mathsf{R}}_{\beta_\eta} (\Lambda_\eta)_\kappa)(\boldsymbol{u}_h)_\kappa$$

$$\quad - \mathbf{1}^{\mathrm{T}} (\tilde{\mathsf{E}}_{\beta_\xi} (\Lambda_\xi)_\kappa + \tilde{\mathsf{E}}_{\beta_\eta} (\Lambda_\eta)_\kappa)(\boldsymbol{u}_h)_\kappa + \mathcal{O}(h^{\tau+1}),$$

or, since $\tilde{\mathsf{Q}}_\xi \mathbf{1} = \tilde{\mathsf{Q}}_\eta \mathbf{1} = \mathbf{0}$ by construction,

$$\int_{\hat{\Gamma}_\kappa^+} \tilde{\boldsymbol{n}} \cdot (\tilde{\boldsymbol{a}} \mathcal{U}_\kappa)\, d\hat{\Gamma} - \mathbf{1}^{\mathrm{T}} \tilde{\mathsf{E}}_{\beta_\xi} (\Lambda_\xi)_\kappa (\boldsymbol{u}_h)_\kappa - \mathbf{1}^{\mathrm{T}} \tilde{\mathsf{E}}_{\beta_\eta} (\Lambda_\eta)_\kappa (\boldsymbol{u}_h)_\kappa = \mathcal{O}(h^{\tau+1}).$$

This concludes the proof. □

Lemma 5 *For each element $\kappa = 1, 2, \ldots, K$, using Assumption 2, the relationships*

$$\mathbf{1}^{\mathrm{T}} \tilde{\mathsf{E}}_{\beta_\xi} (\Lambda_\xi)_\kappa (\boldsymbol{u}_h)_\kappa = \int_{\hat{\Gamma}_\kappa^{\beta_\xi}} \tilde{\boldsymbol{n}} \cdot (\tilde{\boldsymbol{a}} \mathcal{U}_\kappa)\, d\hat{\Gamma} + \mathcal{O}(h^{\tau+1})$$

$$\mathbf{1}^{\mathrm{T}} \tilde{\mathsf{E}}_{\beta_\eta} (\Lambda_\eta)_\kappa (\boldsymbol{u}_h)_\kappa = \int_{\hat{\Gamma}_\kappa^{\beta_\eta}} \tilde{\boldsymbol{n}} \cdot (\tilde{\boldsymbol{a}} \mathcal{U}_\kappa)\, d\hat{\Gamma} + \mathcal{O}(h^{\tau+1})$$

hold, where $\mathcal{U}_\kappa \in C^{\tau+1}(\hat{\Omega}_\kappa)$.

Proof From Lemma 4 we have

$$\underbrace{(\mathbf{1}^{\mathrm{T}} \tilde{\mathsf{E}}_{\beta_\xi} (\Lambda_\xi)_\kappa (\boldsymbol{u}_h)_\kappa - \int_{\hat{\Gamma}_\kappa^{\beta_\xi}} \tilde{\boldsymbol{n}} \cdot (\tilde{\boldsymbol{a}} \mathcal{U}_\kappa)\, d\hat{\Gamma})}_{\text{Term \#1}}$$

$$+ \underbrace{(\mathbf{1}^{\mathrm{T}} \tilde{\mathsf{E}}_{\beta_\eta} (\Lambda_\eta)_\kappa (\boldsymbol{u}_h)_\kappa - \int_{\hat{\Gamma}_\kappa^{\beta_\eta}} \tilde{\boldsymbol{n}} \cdot (\tilde{\boldsymbol{a}} \mathcal{U}_\kappa)\, d\hat{\Gamma})}_{\text{Term \#2}}$$

$$= \mathcal{O}(h^{\tau+1}).$$

However, note that Term #1 is an error term that is only a function of ξ, while Term #2 is an error term that is only a function of η. We thus conclude that

$$\mathbf{1}^{\mathrm{T}} \tilde{\mathsf{E}}_{\beta_\xi} (\Lambda_\xi)_\kappa (\boldsymbol{u}_h)_\kappa = \int_{\hat{\Gamma}_\kappa^{\beta_\xi}} \tilde{\boldsymbol{n}} \cdot (\tilde{\boldsymbol{a}} \mathcal{U}_\kappa)\, d\hat{\Gamma} + \mathcal{O}(h^{\tau+1})$$

$$\mathbf{1}^{\mathrm{T}} \tilde{\mathsf{E}}_{\beta_\eta} (\Lambda_\eta)_\kappa (\boldsymbol{u}_h)_\kappa = \int_{\hat{\Gamma}_\kappa^{\beta_\eta}} \tilde{\boldsymbol{n}} \cdot (\tilde{\boldsymbol{a}} \mathcal{U}_\kappa)\, d\hat{\Gamma} + \mathcal{O}(h^{\tau+1}),$$

as desired. □

Combining the preceding lemmas gives the following result.

Theorem 4 *Let $(\boldsymbol{u}_h)_\kappa \subset \boldsymbol{u}_h$ be the discrete solution that satisfies (21) for $\kappa = 1, 2, \ldots, K$. Furthermore, assume that $\mathcal{U}_\kappa \in C^{\tau+1}(\hat{\Omega}_\kappa)$. Then, using Assumption 2, $\mathcal{I}_h(\boldsymbol{u}_h)$, defined by (22),*

$$\mathcal{I}_h(\boldsymbol{u}_h) = \sum_{\gamma \subset \Gamma^+} \left(\psi^+ \mathbf{1}^{\mathrm{T}} \tilde{\mathsf{E}}_{\hat{\gamma}} (\boldsymbol{u}_h)_\kappa \right),$$

is a degree τ and order $\tau + 1$ approximation of $\mathcal{I}(\mathcal{U})$, defined by (20),

$$\mathcal{I}(\mathcal{U}) = \sum_{\gamma \subset \Gamma^+} \left(\oint_{\hat{\gamma}} \psi^+ \tilde{\boldsymbol{n}} \cdot (\tilde{\boldsymbol{a}} \mathcal{U}_\kappa) \, d\hat{\Gamma} \right).$$

Proof Subtracting (22) from (20) gives

$$\mathcal{I}(\mathcal{U}) - \mathcal{I}_h(\boldsymbol{u}_h)$$
$$= \sum_{\gamma \subset \Gamma^+} \left(\oint_{\hat{\gamma}} \psi^+ \tilde{\boldsymbol{n}} \cdot (\tilde{\boldsymbol{a}} \mathcal{U}_\kappa) \, d\hat{\Gamma} - \psi^+ \mathbf{1}^{\mathrm{T}} \tilde{\mathsf{E}}_{\hat{\gamma}} (\boldsymbol{u}_h)_\kappa \right).$$

However, for every $\gamma \subset \Gamma^+$, either

$$\oint_{\hat{\gamma}} \psi^+ \tilde{\boldsymbol{n}} \cdot (\tilde{\boldsymbol{a}} \mathcal{U}_\kappa) \, d\hat{\Gamma} - \psi^+ \mathbf{1}^{\mathrm{T}} \tilde{\mathsf{E}}_{\hat{\gamma}} (\boldsymbol{u}_h)_\kappa$$
$$= \psi^+ \left(\int_{\hat{\Gamma}_\kappa^{\beta_\xi}} \tilde{\boldsymbol{n}} \cdot (\tilde{\boldsymbol{a}} \mathcal{U}_\kappa) \, d\hat{\Gamma} - \mathbf{1}^{\mathrm{T}} \tilde{\mathsf{E}}_{\beta_\xi} (\Lambda_\xi)_\kappa (\boldsymbol{u}_h)_\kappa \right)$$

or

$$\oint_{\hat{\gamma}} \psi^+ \tilde{\boldsymbol{n}} \cdot (\tilde{\boldsymbol{a}} \mathcal{U}_\kappa) \, d\hat{\Gamma} - \psi^+ \mathbf{1}^{\mathrm{T}} \tilde{\mathsf{E}}_{\hat{\gamma}} (\boldsymbol{u}_h)_\kappa$$
$$= \psi^+ \left(\int_{\hat{\Gamma}_\kappa^{\beta_\eta}} \tilde{\boldsymbol{n}} \cdot (\tilde{\boldsymbol{a}} \mathcal{U}_\kappa) \, d\hat{\Gamma} - \mathbf{1}^{\mathrm{T}} \tilde{\mathsf{E}}_{\beta_\eta} (\Lambda_\eta)_\kappa (\boldsymbol{u}_h)_\kappa \right).$$

Furthermore, from Lemma 5, we have

$$\int_{\hat{\Gamma}_\kappa^{\beta_\xi}} \tilde{\boldsymbol{n}} \cdot (\tilde{\boldsymbol{a}} \mathcal{U}_\kappa) \, d\hat{\Gamma} - \mathbf{1}^{\mathrm{T}} \tilde{\mathsf{E}}_{\beta_\xi} (\Lambda_\xi)_\kappa (\boldsymbol{u}_h)_\kappa = \mathcal{O}(h^{\tau+1})$$
$$\int_{\hat{\Gamma}_\kappa^{\beta_\eta}} \tilde{\boldsymbol{n}} \cdot (\tilde{\boldsymbol{a}} \mathcal{U}_\kappa) \, d\hat{\Gamma} - \mathbf{1}^{\mathrm{T}} \tilde{\mathsf{E}}_{\beta_\eta} (\Lambda_\eta)_\kappa (\boldsymbol{u}_h)_\kappa = \mathcal{O}(h^{\tau+1}).$$

Therefore,

$$\mathcal{I}(\mathcal{U}) - \mathcal{I}_h(\boldsymbol{u}_h)$$
$$= \sum_{\gamma \subset \Gamma^+} \left(\oint_{\hat{\gamma}} \psi^+ \tilde{\boldsymbol{n}} \cdot (\tilde{\boldsymbol{a}} \mathcal{U}_\kappa) \, d\hat{\Gamma} - \psi^+ \mathbf{1}^{\mathrm{T}} \tilde{\mathsf{E}}_{\hat{\gamma}} (\boldsymbol{u}_h)_\kappa \right)$$
$$= \mathcal{O}(h^{\tau+1}),$$

as desired. $\square$

Therefore, we see that the one-dimensional analysis can be extended to multiple dimensions.

4.5 Time-dependent discretization

Here we briefly describe the extension to a time-dependent discretization. Consider the two-dimensional linear convection equation with periodic boundary conditions

$$
\begin{aligned}
&\frac{\partial \mathcal{U}}{\partial t} + \nabla \cdot (\boldsymbol{a}\mathcal{U}) = 0 \quad \forall (x,y) \in \Omega = [\alpha_x, \beta_x] \times [\alpha_y, \beta_y], \quad t \geq 0, \\
&\quad \mathcal{U}(x, y, t = 0) = \mathcal{U}_0(x,y) \\
&\mathcal{U}(x = \alpha_x, y, t) = \mathcal{U}(x = \beta_x, y, t) \\
&\mathcal{U}(x, y = \alpha_y, t) = \mathcal{U}(x, y = \beta_y, t).
\end{aligned}
\tag{23}
$$

Transforming this to the reference element gives, on the κth element,

$$
\mathcal{J}_\kappa \frac{\partial \mathcal{U}_\kappa}{\partial t} + \tilde{\nabla} \cdot (\tilde{\boldsymbol{a}}\mathcal{U}) = 0.
\tag{24}
$$

The discretization of (24), using upwind SATs, is given by

$$
\begin{aligned}
\mathsf{J}_\kappa \frac{d(\boldsymbol{u}_h)_\kappa}{dt} + \tilde{\mathsf{D}}_\xi (\Lambda_\xi)_\kappa (\boldsymbol{u}_h)_\kappa + \tilde{\mathsf{D}}_\eta (\Lambda_\eta)_\kappa (\boldsymbol{u}_h)_\kappa = \\
- \tilde{\mathsf{H}}^{-1} \tilde{\mathsf{R}}_{\alpha_\xi}^{\mathsf{T}} \tilde{\mathsf{H}}_\xi^\perp (\tilde{\mathsf{R}}_{\alpha_\xi}(\Lambda_\xi)_\kappa (\boldsymbol{u}_h)_\kappa - (\lambda_\xi \mathcal{U}_{\text{West}})_\kappa) \\
- \tilde{\mathsf{H}}^{-1} \tilde{\mathsf{R}}_{\alpha_\eta}^{\mathsf{T}} \tilde{\mathsf{H}}_\eta^\perp (\tilde{\mathsf{R}}_{\alpha_\eta}(\Lambda_\eta)_\kappa (\boldsymbol{u}_h)_\kappa - (\lambda_\eta \mathcal{U}_{\text{South}})_\kappa).
\end{aligned}
$$

We note that this two-dimensional problem is a time-dependent problem; however the theory developed thus far extends to time-dependent problems in a straightforward manner. Specifically, time-dependent functionals can be shown to superconverge if the corresponding steady problem, obtained by setting $d\mathcal{U}/dt = 0$, is dual consistent [1]. Therefore, although the theory in this paper has focused on steady problems, the results are immediately applicable to time-dependent problems as well.

5 Main results

Here we verify the theory in the preceding section using one- and two-dimensional numerical examples.

5.1 Two-dimensional quadrature

We can confirm the quadrature accuracy of different generalized SBP operators numerically by examining a two-dimensional quadrature on a curvilinear domain. We take the test problem from Section 4.2 of [21] and restate it here for completeness. Consider the domain

$$
\Omega = \{(x,y) \in \mathbb{R}^2 \mid 1 \leq xy \leq 3, 1 \leq x^2 - y^2 \leq 4\},
$$

and the integral

$$l = \int_{\Omega} (x^2 + y^2) e^{\frac{1-x^2+y^2}{3}} \sin\left(\frac{xy-1}{2}\right) d\Omega \qquad (25)$$
$$= 3(1 - e^{-1})(1 - \cos(1)).$$

We generate the domain Ω by mapping the unit square $(\bar{\bar{x}}, \bar{\bar{y}}) \in [0,1] \times [0,1]$ to Ω as follows

$$\bar{\bar{x}} = \frac{x^2 - y^2 - 1}{3} \quad \text{and} \quad \bar{\bar{y}} = \frac{xy - 1}{2}.$$

To compute (25) numerically, we partition the domain with K nonoverlapping elements. Figure 1 shows the grid for $K = 64$ using the $p = 3$ Legendre-Gauss-Lobatto (LGL) nodes in each element. We note here that although $\bar{\bar{x}} = \bar{\bar{x}}(x, y)$ and $\bar{\bar{y}} = \bar{\bar{y}}(x, y)$ are polynomial functions, $x = x(\bar{\bar{x}}, \bar{\bar{y}})$ and $y = y(\bar{\bar{x}}, \bar{\bar{y}})$ are not. This means that the geometry representation in each element is not a polynomial; however the geometry in each element corresponds to the analytical geometry.
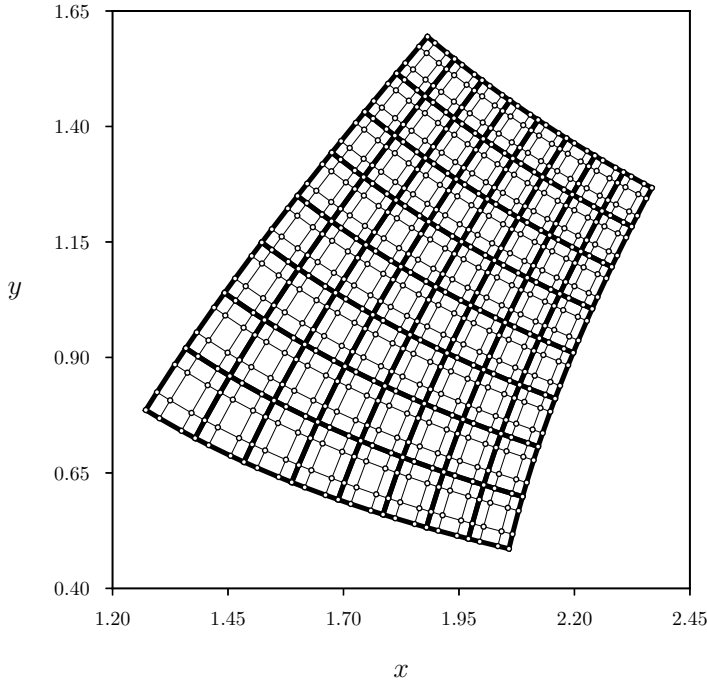
Fig. 1: Example grid for Ω with $K = 64$ nonoverlapping elements. The $p = 3$ LGL nodes are used in each element.

For a given K, the approximation of (25) is summed over all elements to obtain

$$l_h = \sum_{\kappa=1}^{K} (\mathsf{J}_\kappa \mathbf{1})^{\mathrm{T}} \tilde{\mathsf{H}} \boldsymbol{f}_\kappa, \tag{26}$$

where $\boldsymbol{f}_\kappa$ is the integrand of (25) computed using the $\boldsymbol{x}_\kappa$ and $\boldsymbol{y}_\kappa$ coordinates for each element and $\tilde{\mathsf{H}} \equiv \mathsf{H}_\xi \otimes \mathsf{H}_\eta$. Here, the entries in $\boldsymbol{f}_\kappa$ are ordered with those in the η direction varying most rapidly. The error associated with the quadrature approximation is computed as $e_K = |l - l_h|$.

Figure 2 plots the quadrature error, e_K, as a function of the element size, $h = 1/\sqrt{K}$, for the operators listed in Table 1. As expected based on Theorem 2, the quadratures computed using the LGL operators, which have $r = \infty > 2p$, all converge at a rate of approximately order $\tau+1$, where $\tau \geq 2p-1$ denotes the degree of the quadrature rule associated with each operator. These results agree with [11].

(a) Legendre-Gauss-Lobatto family (b) Legendre-Gauss family
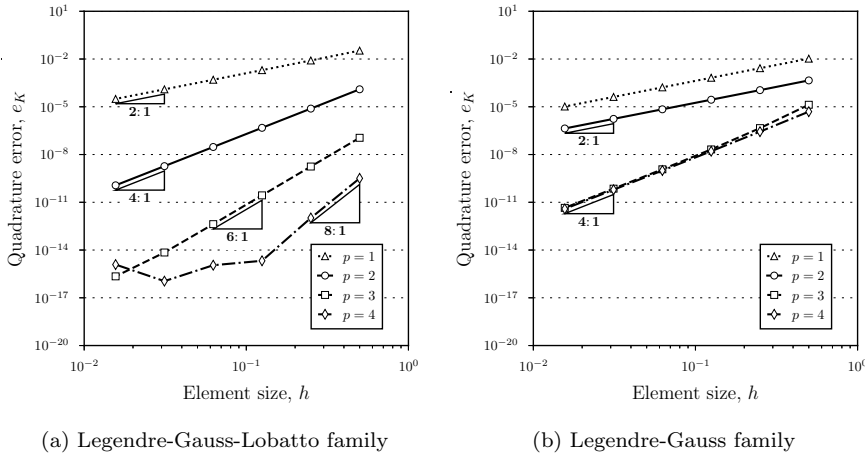
Fig. 2: Convergence of the quadrature error when using the generalized SBP operators in Table 1 to approximate (25).

In contrast, the LG operators all converge at rates less than $2p$, which is also expected since for these operators $r = p < 2p$, the Jacobian is computed using the same SBP operator associated with the norm, and the geometry representation is nonpolynomial. Specifically, there is an even-odd convergence pattern associated with the LG operators. The even-degree LG operators converge at a rate of p while the odd-degree LG operators converge at a rate of approximately $p+1$. This even-odd quadrature convergence behaviour can be explained by considering the interactions between the leading truncation error terms associated with the respective even- and odd-degree LG projection operators. Consider decomposing E_ξ in terms of the projection operators $\boldsymbol{t}_{\alpha_\xi}$

LGp1	i	0	1	2					
	j	3	2	1					
	i+j	$\boxed{3}$	$\boxed{3}$	$\boxed{3}$					
LGp2	i	0	1	2	3	4			
	j	3	4	3	0	1			
	i+j	$\boxed{3}$	5	5	$\boxed{3}$	5			
LGp3	i	0	1	2	3	4	5	6	
	j	5	4	5	4	1	0	1	
	i+j	$\boxed{5}$	$\boxed{5}$	7	7	$\boxed{5}$	$\boxed{5}$	7	
LGp4	i	0	1	2	3	4	5	6	7	8
	j	5	6	5	6	5	0	1	0	1
	i+j	$\boxed{5}$	7	7	9	9	$\boxed{5}$	7	7	9

Table 2: Values of i, j, and $i + j$ when the first nonzero value of e_{E_ξ} occurs. The values of i and j in (29) are increased with j running first.

and $\boldsymbol{t}_{\beta_\xi}$

$$\mathsf{E}_\xi = \boldsymbol{t}_{\beta_\xi}\boldsymbol{t}_{\beta_\xi}^{\mathrm{T}} - \boldsymbol{t}_{\alpha_\xi}\boldsymbol{t}_{\alpha_\xi}^{\mathrm{T}}. \tag{27}$$

Next, recall the accuracy condition on E_ξ from Definition 1. Namely, for some $\hat{\Omega}_\xi \in [\alpha_\xi, \beta_\xi]$, we have

$$\left(\boldsymbol{\xi}^i\right)^{\mathrm{T}}\mathsf{E}_\xi\boldsymbol{\xi}^j = \beta_\xi^{i+j} - \alpha_\xi^{i+j}, \quad i,j,=0,1,\dots r, r \geq p. \tag{28}$$

To make our analysis concrete, we take $[\alpha_\xi, \beta_\xi] = [-1, 1]$. Substituting $\hat{\Omega}_\xi$, i.e., $\alpha_\xi = -1$ and $\beta_\xi = 1$, into (28) and rearranging terms gives us an expression for the error in E_ξ, e_{E_ξ}, for different values of i and j.

$$e_{\mathsf{E}_\xi} = \left(\boldsymbol{\xi}^i\right)^{\mathrm{T}}\mathsf{E}_\xi\boldsymbol{\xi}^j - (1)^{i+j} + (-1)^{i+j}. \tag{29}$$

For LG operators, based on (28), (29) will be equal to zero for $i, j \leq r$. Therefore, we are interested in the behaviour of (29) when $i, j > r$. Table 2 gives the values of i, j, and $i + j$ when the first nonzero value of e_{E_ξ} (i.e., (29)) occurs. For each operator, the minimum value of $i + j$ is $\boxed{\text{boxed}}$. For the odd-degree LG operators, the minimum value of $i+j$ is equal to $p+2$. For the even-degree LG operators, the minimum value of $i + j$ is equal to $p + 1$. To understand why this pattern occurs, we can examine (29) for the minimum values of $i+j$ for each LG operator, as reported in Table 2.

From Table 2, the minimum value of $i + j$ occurs for each operator when $i = 0$. Therefore, we substitute $i = 0$ and (27) into (29), this gives

$$\begin{aligned}
e_{\mathsf{E}_\xi}|_{i=0} &= \left(\boldsymbol{\xi}^0\right)^{\mathrm{T}}\mathsf{E}_\xi\boldsymbol{\xi}^j - (1)^{0+j} + (-1)^{0+j} \\
&= \mathbf{1}^{\mathrm{T}}(\boldsymbol{t}_{\beta_\xi}\boldsymbol{t}_{\beta_\xi}^{\mathrm{T}} - \boldsymbol{t}_{\alpha_\xi}\boldsymbol{t}_{\alpha_\xi}^{\mathrm{T}})\boldsymbol{x}^j - (1)^j + (-1)^j \\
&= \boldsymbol{t}_{\beta_\xi}^{\mathrm{T}}\boldsymbol{\xi}^j - \boldsymbol{t}_{\alpha_\xi}^{\mathrm{T}}\boldsymbol{\xi}^j - 1 + (-1)^j.
\end{aligned}$$

Operator	j	$e_{\mathsf{E}_\xi}\vert_{i=0}$	$e_{\boldsymbol{t}_{\beta_\xi}}$	$e_{\boldsymbol{t}_{\alpha_\xi}}$
LGp1	0	$0.00000e+00$	$-2.22045e-16$	$-2.22045e-16$
$j=r$	1	$-1.11022e-15$	$-2.22045e-16$	$2.22045e-16$
$j=2p$	2	$0.00000e+00$	$\boxed{-6.66667e-01}$	$\boxed{-6.66667e-01}$
	3	$\boxed{-1.33333e+00}$	$-6.66667e-01$	$6.66667e-01$
LGp2	0	$0.00000e+00$	$0.00000e+00$	$0.00000e+00$
	1	$8.88178e-16$	$0.00000e+00$	$0.00000e+00$
$j=r$	2	$0.00000e+00$	$2.22045e-16$	$2.22045e-16$
	3	$\boxed{-8.00000e-01}$	$\boxed{-4.00000e-01}$	$\boxed{4.00000e-01}$
$j=2p$	4	$0.00000e+00$	$-4.00000e-01$	$-4.00000e-01$
LGp3	0	$0.00000e+00$	$0.00000e+00$	$0.00000e+00$
	1	$0.00000e+00$	$-5.55112e-16$	$5.55112e-16$
	2	$0.00000e+00$	$0.00000e+00$	$0.00000e+00$
$j=r$	3	$0.00000e+00$	$-4.44089e-16$	$4.44089e-16$
	4	$0.00000e+00$	$\boxed{-2.28571e-01}$	$\boxed{-2.28571e-01}$
	5	$\boxed{-4.57143e-01}$	$-2.28571e-01$	$2.28571e-01$
$j=2p$	6	$0.00000e+00$	$-4.24490e-01$	$-4.24490e-01$
LGp4	0	$2.22045e-16$	$0.00000e+00$	$2.22045e-16$
	1	$0.00000e+00$	$0.00000e+00$	$2.22045e-16$
	2	$1.11022e-16$	$-2.22045e-16$	$-2.22045e-16$
	3	$-4.44089e-16$	$-2.22045e-16$	$4.44089e-16$
$j=r$	4	$1.11022e-16$	$-1.11022e-16$	$-1.11022e-16$
	5	$\boxed{-2.53968e-01}$	$\boxed{-1.26984e-01}$	$\boxed{1.26984e-01}$
	6	$1.11022e-16$	$-1.26984e-01$	$-1.26984e-01$
	7	$-5.36155e-01$	$-2.68078e-01$	$2.68078e-01$
$j=2p$	8	$1.11022e-16$	$-2.68078e-01$	$-2.68078e-01$

Table 3: Interpolation/extrapolation error associated with the Legendre-Gauss (LG) family of operators.

Note also that $\mathbf{1}^{\mathrm{T}}\boldsymbol{t}_{\beta_\xi} = \mathbf{1}^{\mathrm{T}}\boldsymbol{t}_{\alpha_\xi} = 1$ since the interpolation/extrapolation operators evaluate the constant function exactly. We now introduce two additional error metrics. Let

$$e_{\boldsymbol{t}_{\beta_\xi}} = \boldsymbol{t}_{\beta_\xi}^{\mathrm{T}}\boldsymbol{\xi}^j - 1, \tag{30}$$

$$e_{\boldsymbol{t}_{\alpha_\xi}} = \boldsymbol{t}_{\alpha_\xi}^{\mathrm{T}}\boldsymbol{\xi}^j - (-1)^j, \tag{31}$$

be the error associated with the interpolation/extrapolation operators $\boldsymbol{t}_{\beta_\xi}$ and $\boldsymbol{t}_{\alpha_\xi}$, respectively. Note that we can recast $e_{\mathsf{E}_\xi}\vert_{i=0}$ in terms of $e_{\boldsymbol{t}_{\beta_\xi}}$ and $e_{\boldsymbol{t}_{\alpha_\xi}}$ as

$$e_{\mathsf{E}_\xi}\vert_{i=0} = e_{\boldsymbol{t}_{\beta_\xi}} - e_{\boldsymbol{t}_{\alpha_\xi}}. \tag{32}$$

Table 3 numerically tabulates these error terms for the LG operators listed in Table 1 for different j.

First note that all error terms are zero (or machine zero) up to $j = r$. This is expected from the accuracy condition on E_ξ associated with Definition 1. Therefore, we expect that $e_{\boldsymbol{t}_{\beta_\xi}}$ and $e_{\boldsymbol{t}_{\alpha_\xi}}$ will be non-zero for $j > r$. The

first nonzero (or nonmachine-zero) values of $e_{\boldsymbol{t}_{\beta_\xi}}$ and $e_{\boldsymbol{t}_{\alpha_\xi}}$ that appear when increasing j from 0 to $2p$ are $\boxed{\text{boxed}}$, and this occurs for each operator when $j = r + 1$. Similarly, the first non-zero value of $e_{\mathsf{E}_\xi}|_{i=0}$ for each operator is $\boxed{\text{boxed}}$. For the even-degree operators, the first non-zero values of $e_{\boldsymbol{t}_{\beta_\xi}}$ and $e_{\boldsymbol{t}_{\alpha_\xi}}$ are equal and opposite in sign, which results in the first non-zero value of $e_{\mathsf{E}_\xi}|_{i=0}$ occurring at $j = r + 1$. In contrast, the first non-zero values of $e_{\boldsymbol{t}_{\beta_\xi}}$ and $e_{\boldsymbol{t}_{\alpha_\xi}}$ are equal and of the same sign, which causes them to cancel when $j = r+1$. As a result of this cancellation, the first non-zero value of $e_{\mathsf{E}_\xi}|_{i=0}$ for the odd-degree operators occurs at $j = r+2$, i.e., one value of j higher than for the even-degree operators. This explains the even-odd quadrature convergence behaviour observed in Figure 2 with the even-degree LG operators converging at a rate of p and the odd-degree LG operators converging at a rate of $p+1$. Essentially, in curvilinear coordinates, when the Jacobian is approximated using the same SBP derivative operator associated with the norm and the geometry representation is either nonpolynomial or of a degree higher than that of the SBP operator, the LG quadrature accuracy is limited by the accuracy of the projection operators, and the even-odd quadrature convergence behaviour is associated with the leading truncation error cancellation of the projection operators that occurs for the odd-degree LG operators.

5.2 Steady one-dimensional boundary-value problem

Consider the steady one-dimensional boundary-value problem

$$\frac{d\mathcal{U}(x)}{dx} = \mathcal{F}(x) \quad \forall x \in \Omega_x = [0,1]$$
$$\mathcal{U}(x = 0) = \sin(1), \tag{33}$$

where the source term,

$$\mathcal{F}(x) = \frac{\pi e^x}{e-1} \cos\left(\frac{\pi e^x - \pi + e - 1}{e-1}\right), \tag{34}$$

gives the steady-state solution

$$\mathcal{U}(x) = \sin\left(\frac{\pi(e^x - 1)}{e-1} + 1\right). \tag{35}$$

Note that this problem is similar to one from [17]. We use the mesh functions, $x = x(\bar{\bar{x}})$, in Table 4 to introduce a nonconstant metric Jacobian into integral functionals on Ω_x, which simulates the effect of a curvilinear coordinate transformation.

Consider the functionals

$$\mathcal{I}(\mathcal{U}) = \int_{\Omega_x} \mathcal{G}\mathcal{U}\, d\Omega_x + (\mathcal{U})|_{x=1} = \sum_{\kappa=1}^{K} \int_{(\hat{\Omega}_\xi)_\kappa} \mathcal{G}_\kappa \mathcal{U}_\kappa \mathcal{J}_\kappa\, d\hat{\Omega}_\xi + (\mathcal{U}_K)|_{\xi=\beta_\xi} \tag{36}$$
$$\approx -0.36537991553426102$$

Polynomial Degree	Mesh Function	Abbreviation
1	$\bar{\bar{x}}$	MFD1
2	$\frac{1}{2}\bar{\bar{x}}^2 + \frac{1}{2}\bar{\bar{x}}$	MFD2
3	$\frac{1}{3}\bar{\bar{x}}^3 + \frac{1}{3}\bar{\bar{x}}^2 + \frac{1}{3}\bar{\bar{x}}$	MFD3
4	$\frac{1}{4}\bar{\bar{x}}^4 + \frac{1}{4}\bar{\bar{x}}^3 + \frac{1}{4}\bar{\bar{x}}^2 + \frac{1}{4}\bar{\bar{x}}$	MFD4
5	$\frac{1}{5}\bar{\bar{x}}^5 + \frac{1}{5}\bar{\bar{x}}^4 + \frac{1}{5}\bar{\bar{x}}^3 + \frac{1}{5}\bar{\bar{x}}^2 + \frac{1}{5}\bar{\bar{x}}$	MFD5
nonpolynomial	$(\exp(4\bar{\bar{x}}) - 1)/(\exp(4) - 1)$	MFNP

Table 4: Mesh functions.

and

$$\mathcal{I}^{\mathrm{bnd}}(\mathcal{U}) = (\mathcal{U})|_{x=1} = (\mathcal{U}_K)|_{\xi=\beta_\xi}$$
$$= -\sin(1), \tag{37}$$

discretized as

$$\mathcal{I}_h(\boldsymbol{u}_h) = \sum_{\kappa=1}^{K} \boldsymbol{g}_\kappa^{\mathrm{T}} \mathsf{H}_\xi \mathsf{J}_\kappa (\boldsymbol{u}_h)_\kappa + \boldsymbol{t}_{\beta_\xi}^{\mathrm{T}} (\boldsymbol{u}_h)_K \tag{38}$$

and

$$\mathcal{I}_h^{\mathrm{bnd}}(\boldsymbol{u}_h) = \boldsymbol{t}_{\beta_\xi}^{\mathrm{T}} (\boldsymbol{u}_h)_K, \tag{39}$$

respectively. Here, $\mathcal{G}(x) = \sin(x+1)$. Note that we have not found a closed form expression for the integral in (36) and have therefore approximated the exact value of this functional using an adaptive Gaussian quadrature method. Furthermore, the functional error is evaluated as the absolute value of the difference between the exact and numerical functionals.

Table 5 tabulates the approximate convergence results when using (38) to discretize (36) with the mesh functions in Table 4. Upwind SATs were used. Figure 3 plots the results when using the nonpolynomial mesh function. Similarly, Figure 4 shows the results when using (39) to approximate (37).

From Table 5, as for the two-dimensional quadrature example, the LGL operators converge at a rate of approximately the quadrature degree, τ, plus one, i.e., $\tau + 1$. In contrast, the LG operators converge at a rate of $\tau + 1$ only when the mesh function is a polynomial whose degree is less than or equal to the degree of the SBP operator used to compute the Jacobian. Note that the ✔-marks indicate superconvergent convergence rates. When a mesh function is used that does not satisfy this condition, the odd- and even-degree LG operators converge at rates of $p + 1$ and p, respectively. These convergence rates are boxed in Table 5 and highlighted using ✗-marks. As before, the even-odd convergence behaviour can be explained by considering the error cancellation associated with the leading truncation error terms of the odd-degree LG projection operators. These observations also hold when the functional consists solely of a boundary term, as exemplified by Figure 4.
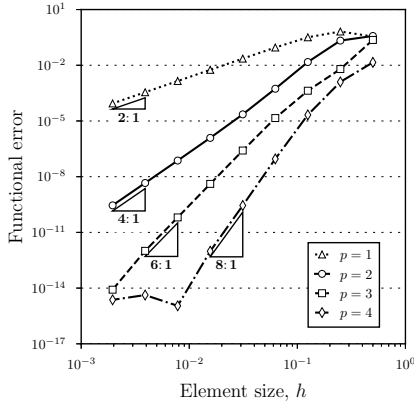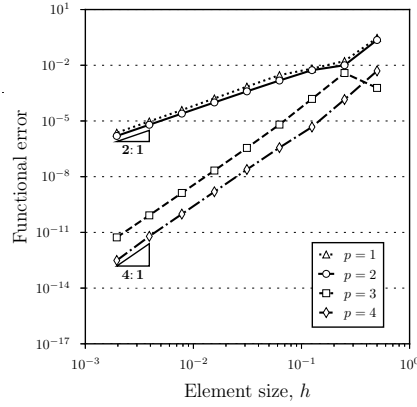
(a) Legendre-Gauss-Lobatto family   (b) Legendre-Gauss family

Fig. 3: Convergence of the functional error when using the generalized SBP operators in Table 1 to approximate (36) with the nonpolynomial mesh function in Table 4.
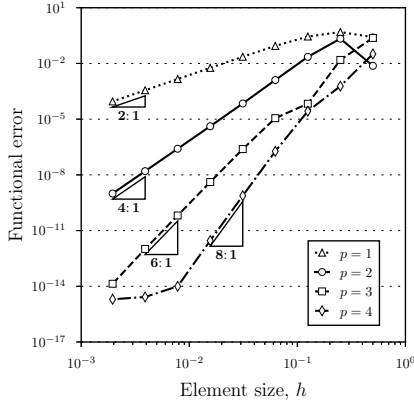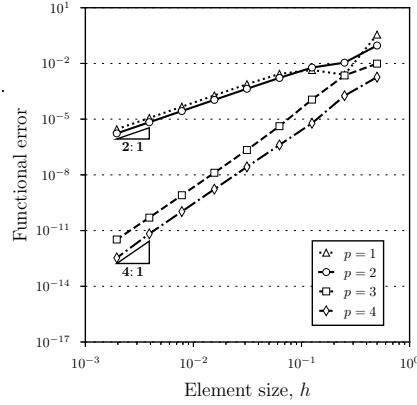
(a) Legendre-Gauss-Lobatto family   (b) Legendre-Gauss family

Fig. 4: Convergence of the functional error when using the generalized SBP operators in Table 1 to approximate (37) with the nonpolynomial mesh function in Table 4.

5.3 Regularity of the mapping

Here, we introduce two additional mesh functions (1) to verify that the interface coupling procedure allows for different mappings in different elements and (2) to verify that a nonpolynomial mapping with C^p continuity leads to similar results as the previously investigated nonpolynomial mapping having

Operator	MFD1	MFD2	MFD3	MFD4	MFD5	MFNP
LGLp1	✔ ∼ 2	✔ ∼ 2	✔ ∼ 2	✔ ∼ 2	✔ ∼ 2	✔ ∼ 2
LGLp2	✔ ∼ 4	✔ ∼ 4	✔ ∼ 4	✔ ∼ 4	✔ ∼ 4	✔ ∼ 4
LGLp3	✔ ∼ 6	✔ ∼ 6	✔ ∼ 6	✔ ∼ 6	✔ ∼ 6	✔ ∼ 6
LGLp4	✔ ∼ 8	✔ ∼ 8	✔ ∼ 8	✔ ∼ 8	✔ ∼ 8	✔ ∼ 8
LGp1	✔ ∼ 4	�’ ∼ 2	✗ ∼ 2	✗ ∼ 2	✗ ∼ 2	✗ ∼ 2
LGp2	✔ ∼ 6	✔ ∼ 6	✗ ∼ 2	✗ ∼ 2	✗ ∼ 2	✗ ∼ 2
LGp3	✔ ∼ 8	✔ ∼ 8	✔ ∼ 8	✗ ∼ 4	✗ ∼ 4	✗ ∼ 4
LGp4	✔ ∼ 10	✔ ∼ 10	✔ ∼ 10	✔ ∼ 10	✗ ∼ 4	✗ ∼ 4

Table 5: Approximate convergence rates when using the generalized SBP operators in Table 1 to approximate (36) via (38) with the mesh functions defined in Table 4. The ✔-marks denote superconvergent rates while the ✗-marks means that superconvergence was not achieved.

C^∞ continuity. To this end, consider the piecewise polynomial mesh function

$$x(\bar{\bar{x}}) = \begin{cases} \bar{\bar{x}}^2 + \frac{1}{2}\bar{\bar{x}} & \bar{\bar{x}} \le \frac{1}{2} \\ \bar{\bar{x}} & \frac{1}{2} \le \bar{\bar{x}}, \end{cases} \tag{40}$$

which is C^0 continuous at $\bar{\bar{x}} = 1/2$, and the nonpolynomial mesh function

$$x(\bar{\bar{x}}) = \left| \bar{\bar{x}} - \frac{1}{3} \right|^3 - \frac{1}{27} + \frac{20\sin(\bar{\bar{x}})}{27\sin(1)}, \tag{41}$$

which is C^2 continuous at $\bar{\bar{x}} = 1/3$.

The convergence of the functional error when using the degree $p = 2$ generalized SBP operators in Table 1 to approximate (36) with the mesh functions defined by (40) and (41) is shown in Figure 5.

When using the piecewise polynomial mesh function having a C^0 continuous point at $\bar{\bar{x}} = 1/2$, our refinement strategy ensures that an element interface is always aligned with the C^0 continuous point. Hence we are still able to achieve a convergence rate of $\tau + 1$ for the degree $p = 2$ LGL operator. Furthermore, the degree of the polynomial on either side of $\bar{\bar{x}} = 1/2$ is less than or equal to two, so the degree $p = 2$ LG operator also achieves a convergence rate of at least $\tau + 1$ when using the piecewise polynomial mesh function. For the nonpolynomial mesh function, the LG operator underconverges in the same manner as observed in the preceding section, and the C^2 continuous point (that always falls within the interior of an element) does not affect the convergence of the degree $p = 2$ LGL operator, as expected.

(a) Mesh function given by (40)   (b) Mesh function given by (41)
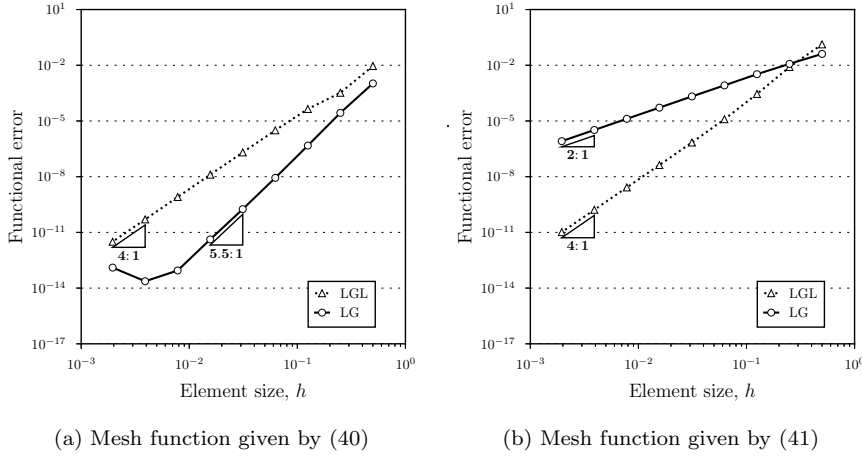
Fig. 5: Convergence of the functional error when using the degree $p = 2$ generalized SBP operators in Table 1 to approximate (36) with the mesh functions defined by (40) and (41).

5.4 Unsteady two-dimensional linear convection equation

Based on the problem formulation introduced in Section 4.5, we use $\Omega = [0,1] \times [0,1]$ with initial condition

$$\mathcal{U}_0(x, y) = \sin(2\pi x) + \sin(2\pi y),$$

and march the numerical solution to a time of $t = 3$ using the fourth-order Runge-Kutta time-marching method with CFL $= 0.5$ [10]. To generate curvilinear grids, we map the unit square $(\bar{\bar{x}}, \bar{\bar{y}}) \in [0,1] \times [0,1]$ to Ω through [10]

$$x = \bar{\bar{x}} + \frac{1}{5} \sin(\pi\bar{\bar{x}}) \sin(\pi\bar{\bar{y}})$$

$$y = \bar{\bar{y}} + \frac{1}{5} \exp(1 - \bar{\bar{y}}) \sin(\pi\bar{\bar{x}}) \sin(\pi\bar{\bar{y}}).$$

An example grid is shown in Figure 6. The continuous functional

$$\mathcal{I}(\mathcal{U}|_{t=3}) = \int_\Omega \mathcal{G}\mathcal{U}|_{t=3} \, d\Omega,$$

with $\mathcal{G} = 1$, is discretized as

$$\mathcal{I}_h(\boldsymbol{u}_h) = \sum_{\kappa=1}^K \boldsymbol{g}_\kappa^{\mathrm{T}} \tilde{\mathsf{H}} \mathsf{J}_\kappa (\boldsymbol{u}_h)_\kappa,$$

where $(\boldsymbol{u}_h)_\kappa$ is the numerical solution on the κth-element at time $t = 3$. The error between the continuous and discrete functionals when using the operators in Table 1 is plotted in Figure 7. Once again, we see that even though the LG
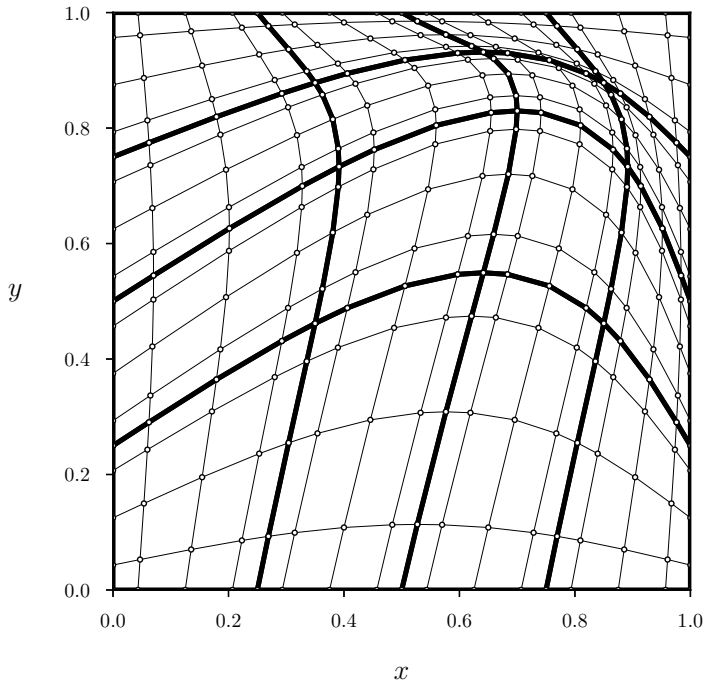
Fig. 6: Example grid for Ω with $K = 16$ nonoverlapping elements. The $p = 4$ LGL nodes are used in each element.

operators typically have better solution accuracy compared to the LGL operators, the functional accuracy is not necessarily more accurate in curvilinear coordinates, depending on the degree of the geometry representation.

6 Conclusions

We have shown that, for tensor-product generalized SBP operators, projection operators of degree $r \geq 2p$ are required to preserve quadrature accuracy and therefore superconvergent functionals in curvilinear coordinates when (1) the Jacobian of the transformation is approximated by the same SBP operator that is associated with the norm and (2) when a higher degree representation of the geometry is used compared to the degree of the SBP operator. Furthermore, when the geometry condition is violated for the LG SBP operators, which have $r = p < 2p$, there is an even-odd quadrature convergence behaviour that can be explained by considering the cancellation of the leading truncation error terms for the LG projection operators associated with the odd-degree LG operators. Numerical examples in one- and two-dimensions were presented verifying the developed theory. Future work will focus on PDEs with diffusion-type terms

(a) Legendre-Gauss-Lobatto family   (b) Legendre-Gauss family
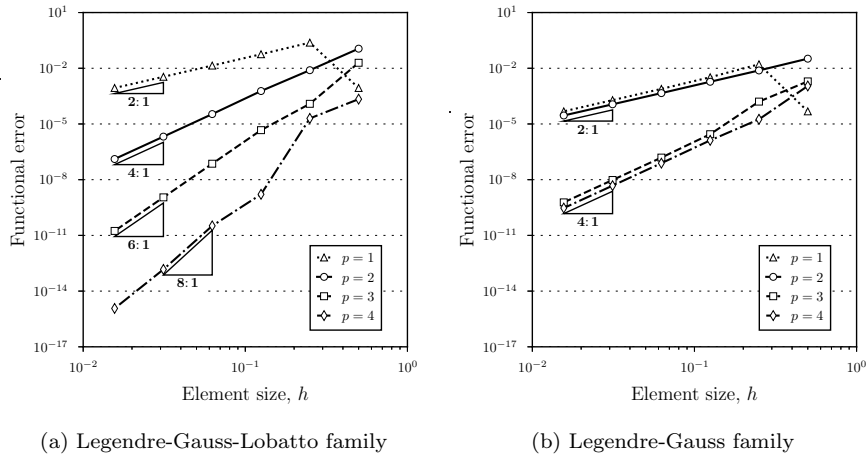
Fig. 7: Convergence of the functional error when using the generalized SBP operators in Table 1 to approximate the discrete functional for the unsteady two-dimensional linear convection equation.

and those that involve nonlinearity. Following [17, 22], extending the proofs to nonlinear problems could potentially be done through Fréchet linearization.

References

1. Berg, J., Nordström, J.: Superconvergent functional output for time-dependent problems using finite differences on summation-by-parts form. Journal of Computational Physics **231**(20), 6846–6860 (2012)
2. Boom, P.D.: High-order implicit time-marching methods for unsteady fluid flow simulation. Ph.D. thesis, University of Toronto (2015)
3. Boom, P.D., Zingg, D.W.: High-order implicit time-marching methods based on generalized summation-by-parts operators. SIAM Journal on Scientific Computing **37**(6), A2682–A2709 (2015)
4. Carpenter, M.H., Gottlieb, D.: Spectral methods on arbitrary grids. Journal of Computational Physics **129**(1), 74–86 (1996)
5. Carpenter, M.H., Gottlieb, D., Abarbanel, S.: Time-stable boundary conditions for finite-difference schemes solving hyperbolic systems: Methodology and application to high-order compact schemes. Journal of Computational Physics **111**, 220–236 (1994)
6. Cockburn, B., Wang, Z.: Adjoint-based, superconvergent Galerkin approximations of linear functionals. Journal of Scientific Computing **73**(2-3), 644–666 (2017)
7. Crean, J., Hicken, J.E., Del Rey Fernández, D.C., Zingg, D.W., Carpenter, M.H.: Entropy-stable summation-by-parts discretization of the Euler equations on general curved elements. Journal of Computational Physics **356**, 410–438 (2018)
8. Del Rey Fernández, D.C.: Generalized summation-by-parts operators for first and second derivatives. Ph.D. thesis, University of Toronto (2015)

9. Del Rey Fernández, D.C., Boom, P.D., Carpenter, M.H., Zingg, D.W.: Extension of tensor-product generalized and dense-norm summation-by-parts operators to curvilinear coordinates. Journal of Scientific Computing **80**(3), 1957–1996 (2019)

10. Del Rey Fernández, D.C., Boom, P.D., Shademan, M., Zingg, D.W.: Numerical investigation of tensor-product summation-by-parts discretization strategies and operators. 55th AIAA Aerospace Sciences Meeting (2017). AIAA paper 2017-0530

11. Del Rey Fernández, D.C., Boom, P.D., Zingg, D.W.: A generalized framework for nodal first derivative summation-by-parts operators. Journal of Computational Physics **266**, 214–239 (2014)

12. Del Rey Fernández, D.C., Hicken, J.E., Zingg, D.W.: Review of summation-by-parts operators with simultaneous approximation terms for the numerical solution of partial differential equations. Computers & Fluids **95**, 171–196 (2014)

13. Funaro, D., Gottlieb, D.: A new method of imposing boundary conditions in pseudospectral approximations of hyperbolic equations. Mathematics of Computation **51**(184), 599–613 (1988)

14. Gassner, G.J.: A skew-symmetric discontinuous Galerkin spectral element discretization and its relation to SBP-SAT finite difference methods. SIAM Journal on Scientific Computing **35**(3), A1233–A1253 (2013)

15. Gassner, G.J., Winters, A.R., Kopriva, D.A.: Split form nodal discontinuous Galerkin schemes with summation-by-parts property for the compressible Euler equations. Journal of Computational Physics **327**, 39–66 (2016)

16. Hartmann, R.: Adjoint consistency analysis of discontinuous Galerkin discretizations. SIAM Journal on Numerical Analysis **45**(6), 2671–2696 (2007)

17. Hicken, J.E.: Output error estimation for summation-by-parts finite-difference schemes. Journal of Computational Physics **231**(9), 3828–3848 (2012)

18. Hicken, J.E., Del Rey Fernández, D.C., Zingg, D.W.: Multidimensional summation-by-parts operators: General theory and application to simplex elements. SIAM Journal on Scientific Computing **38**(4), A1935–A1958 (2016)

19. Hicken, J.E., Zingg, D.W.: Parallel Newton-Krylov solver for the Euler equations discretized using simultaneous approximation terms. AIAA Journal **46**(11), 2773–2786 (2008)

20. Hicken, J.E., Zingg, D.W.: Superconvergent functional estimates from summation-by-parts finite-difference discretizations. SIAM Journal on Scientific Computing **33**(2), 893–922 (2011)

21. Hicken, J.E., Zingg, D.W.: Summation-by-parts operators and high-order quadrature. Journal of Computational and Applied Mathematics **237**(1), 111–125 (2013)

22. Hicken, J.E., Zingg, D.W.: Dual consistency and functional accuracy: a finite-difference perspective. Journal of Computational Physics **256**, 161–182 (2014)

23. Hunter, J.D.: Matplotlib: A 2d graphics environment. Computing in Science & Engineering **9**(3), 90–95 (2007)

24. Koepf, W.: Hypergeometric Summation. Universitext. Springer London, London (2014)

25. Kreiss, H.O., Scherer, G.: Finite element and finite difference methods for hyperbolic partial differential equations. In: Mathematical Aspects of Finite Elements in Partial Differential Equations, pp. 195–212. Academic Press, New York/London (1974)

26. Krivodonova, L., Xin, J., Remacle, J.F., Chevaugeon, N., Flaherty, J.E.: Shock detection and limiting with discontinuous Galerkin methods for hyperbolic conservation laws. Applied Numerical Mathematics **48**(3-4), 323–338 (2004)

27. Loken, C., Gruner, D., Groer, L., Peltier, R., Bunn, N., Craig, M., Henriques, T., Dempsey, J., Yu, C.H., Chen, J., Dursi, L.J., Chong, J., Northrup, S., Pinto, J., Knecht, N., Zon, R.V.: SciNet: Lessons learned from building a power-efficient top-20 system and data centre. Journal of Physics: Conference Series **256**, 012026 (2010)

28. Lu, J.C.C.: An a posteriori error control framework for adaptive precision optimization using discontinuous Galerkin finite element method. Ph.D. thesis, Massachusetts Institute of Technology (2005)

29. Nordström, J.: Conservative finite difference formulations, variable coefficients, energy estimates and artificial dissipation. Journal of Scientific Computing **29**(3), 375–404 (2006)

30. Osusky, M., Zingg, D.W.: Parallel Newton-Krylov-Schur flow solver for the Navier-Stokes equations. AIAA journal **51**(12), 2833–2851 (2013)

31. Ranocha, H.: Generalised summation-by-parts operators and variable coefficients. Journal of Computational Physics **362**, 20–48 (2018)
32. Ranocha, H., Öffner, P., Sonar, T.: Summation-by-parts operators for correction procedure via reconstruction. Journal of Computational Physics **311**, 299–328 (2016)
33. Svärd, M., Carpenter, M.H., Nordström, J.: A stable high-order finite difference scheme for the compressible Navier-Stokes equations, far-field boundary conditions. Journal of Computational Physics **225**(1), 1020–1038 (2007)
34. Svärd, M., Nordström, J.: Review of summation-by-parts schemes for initial-boundary-value problems. Journal of Computational Physics **268**, 17–38 (2014)
35. Thomas, P.D., Lombard, C.K.: Geometric conservation law and its application to flow computations on moving grids. AIAA Journal **17**(10), 1030–1037 (1979)